CRREL Report 84-8

April 1984

Mechanical properties of multi-year sea ice
Testing techniques

M. Mellor, G.F.N. Cox and H. Bosworth

REPORT DOCUMENTATION PAGE

READ INSTRUCTIONS BEFORE COMPLETING FORM

1. REPORT NUMBER: CRREL Report 84-8
2. GOVT ACCESSION NO.:
3. RECIPIENT'S CATALOG NUMBER:

4. TITLE (and Subtitle): MECHANICAL PROPERTIES OF MULTI-YEAR SEA ICE
Testing Techniques

5. TYPE OF REPORT & PERIOD COVERED:
6. PERFORMING ORG. REPORT NUMBER:

7. AUTHOR(s): M. Mellor, G.F.N. Cox and H. Bosworth

8. CONTRACT OR GRANT NUMBER(s):

9. PERFORMING ORGANIZATION NAME AND ADDRESS
U.S. Army Cold Regions Research and Engineering Laboratory
Hanover, New Hampshire 03755

10. PROGRAM ELEMENT, PROJECT, TASK AREA & WORK UNIT NUMBERS:

11. CONTROLLING OFFICE NAME AND ADDRESS
Shell Development Company, Houston, Texas 77001 and
U.S. Geological Survey (now Minerals Management Service)
Reston, Virginia 22092

12. REPORT DATE: April 1984
13. NUMBER OF PAGES: 43

14. MONITORING AGENCY NAME & ADDRESS (if different from Controlling Office):

15. SECURITY CLASS. (of this report): Unclassified
15a. DECLASSIFICATION/DOWNGRADING SCHEDULE:

16. DISTRIBUTION STATEMENT (of this Report)

Approved for public release; distribution unlimited.

17. DISTRIBUTION STATEMENT (of the abstract entered in Block 20, if different from Report)

18. SUPPLEMENTARY NOTES

19. KEY WORDS (Continue on reverse side if necessary and identify by block number)

Ice
Ice properties
Mechanical properties
Sea ice
Test techniques

20. ABSTRACT (Continue on reverse side if necessary and identify by block number)

This report describes the equipment and procedures that were used for acquiring, preparing and testing samples of multi-year sea ice. Techniques and procedures are discussed for testing ice samples in compression and tension at constant strain rates and constant loads, as well as in a conventional triaxial cell. A detailed account is given of the application and measurement of forces and displacements on the ice test specimens under these different loading conditions.

PREFACE

This report was prepared by Dr. Malcolm Mellor, Research Physical Scientist, of the Experimental Engineering Division, Dr. Gordon F.N. Cox, Research Geophysicist, and Hazen W. Bosworth, Physical Science Technician, both of the Snow and Ice Branch, Research Division, U.S. Army Cold Regions Research and Engineering Laboratory. The study was sponsored by the Shell Development Company and the Minerals Management Service of the Department of the Interior with support from the Amoco Production Company, Arco Oil and Gas Company, Chevron Oil Field Research Company, Exxon Production Research Company, Gulf Research and Development Company, Mitsui Engineering and Shipbuilding Company, the National Science Foundation, Sohio Petroleum Company, Texaco, the U.S. Department of Energy and the U.S. Coast Guard.

The authors thank Jacqueline Richter-Menge of CRREL and Dr. Jim Dorris of Shell Development Company for technically reviewing the manuscript of this report.

CONTENTS

ILLUSTRATIONS

Figure

MECHANICAL PROPERTIES OF MULTI-YEAR SEA ICE
TESTING TECHNIQUES

M. Mellor, G.F.N. Cox and H. Bosworth

INTRODUCTION

The CRREL study "Mechanical Properties of Multi-Year Sea Ice" involved a collaboration between industry and government that is unusual in the U.S. The intent was to avoid wasteful duplication and disputes in the generation of basic arctic design data by conducting careful tests in an impartial government research laboratory with financial support from a group of oil companies and government regulatory agencies.

The CRREL research group sought to employ testing techniques that would stand up to critical professional scrutiny, avoiding use of some older flawed procedures. The contract could not provide for unlimited development work on testing techniques, and thus most tests were run with equipment and procedures that fall short of the ideal. However, the methods used are believed to be fully adequate for studying the highly variable and strongly inhomogeneous multi-year ridge ice samples obtained from the field sampling programs.

This report describes the equipment and procedures that were used for acquiring, preparing and testing samples of multi-year sea ice in Phase I of the project. A detailed account is given in order to permit critical evaluation of the test data, and also to facilitate future refinements of testing techniques. The test results from this study are given in a companion report "Mechanical Properties of Multi-Year Sea Ice, Phase I: Test Results" (Cox et al. 1984).

TEST MATERIAL AND TEST SPECIMENS

Test material

The study was directed towards developing an understanding of the structure and strength of ice samples obtained from multi-year pressure ridges in the Beaufort Sea. This material is of relatively low salinity and is highly variable in composition and structure. Salinity typically ranges from 0.5 to 2.0‰. Bulk density is in the range 0.860 to 0.915 Mg/m^3, and porosity is in the range 15 to 70‰. The main bulk of the multi-year ice consists of rafted and pressured accumulations of what was once first-year sheet ice, which has been subject to melting and refreezing, brine drainage, and meltwater infiltration. The multi-year ice samples also contain ice formed from snow, from accumulations of frazil, and from melt ponds. Pores contain both brine and air; near the upper surfaces of the pressure ridges the pores can be very large—1 cm or more in diameter. Grain sizes range from less than 1 mm for snow ice and frazil ice to about 15 mm for columnar ice and meltwater ice.

Required dimensions for test specimens

In materials such as rock, concrete and ice the effective strength tends to decrease as the stressed volume of material increases, since the probability of encountering larger, and therefore more critical, flaws increases with the stressed volume. It is obviously impractical to test enormous specimens in the laboratory, but for granular materials it is generally accepted that test specimens should be large relative to the grain size so as to give representative data for the bulk material. The practical question is, How small can a specimen be?

Hawkes and Mellor (1970) considered the disturbance of grain stress by proximity to a free surface of the specimen, and concluded that the minimum linear dimension of any test specimen should be at least 10 times the grain size, and preferably 20 times. In a recent study on ice Jones and Chew (1981) confirmed this finding experimentally for uniaxial compression tests, recommending that the specimen diameter be at least 12 times the grain size. In this program it was expected that the average grain size of ice samples might be up to about 10 mm, so it

was felt that the specimen diameter ought to be at least 10 cm. The diameter of the drilled core has to be slightly larger than the finished diameter to allow for machining. Compared with core sizes for existing ice drills, this diameter is large, and there is not much latitude for going beyond the minimum requirements.

The required length of the specimen L is some multiple of the diameter D. It is obviously undesirable to have L/D very big, as the specimen would become prone to buckling, and there would be a heavy demand for long sections of unflawed core. At the other extreme, L/D cannot be too small because the stress field in a cylindrical specimen is inevitably perturbed in the vicinity of the loading platens. Thus, the specimen has to be long enough to give a midsection that has a stress field close to uniaxial over a length $L/D \approx 1$. Many theoretical and experimental studies have shown that L/D for loading with typical platens should not be less than 2 and probably not more than 3. A value $L/D = 2.5$ is widely recognized as a sound choice [see Hawkes and Mellor (1970) for a review of relevant studies].

The final choice for the nominal dimensions of test specimens to be used in compression tests was $D = 4$ in. (102 mm), $L = 10$ in. (254 mm). It was recognized that tension specimens might have to be machined to a dumbbell shape with the diameter of the midsection somewhat less than 4 in., but this was judged to be acceptable.

ACQUISITION AND PREPARATION OF SPECIMENS

Field core sampling

If 4 in. was to be the finished diameter for specimens, the core diameter had to be slightly greater than 4 in., the actual core diameter being determined by the design of the coring drill. Since the core barrel of the drill was to be made from spun fiberglass tubing, stock sizes of this material determined the internal diameter of the core barrel, which turned out to be 4.25 in. (108 mm).

The basic coring auger (Fig. 1) is described briefly by Cox et al. (1984) and in detail by Rand

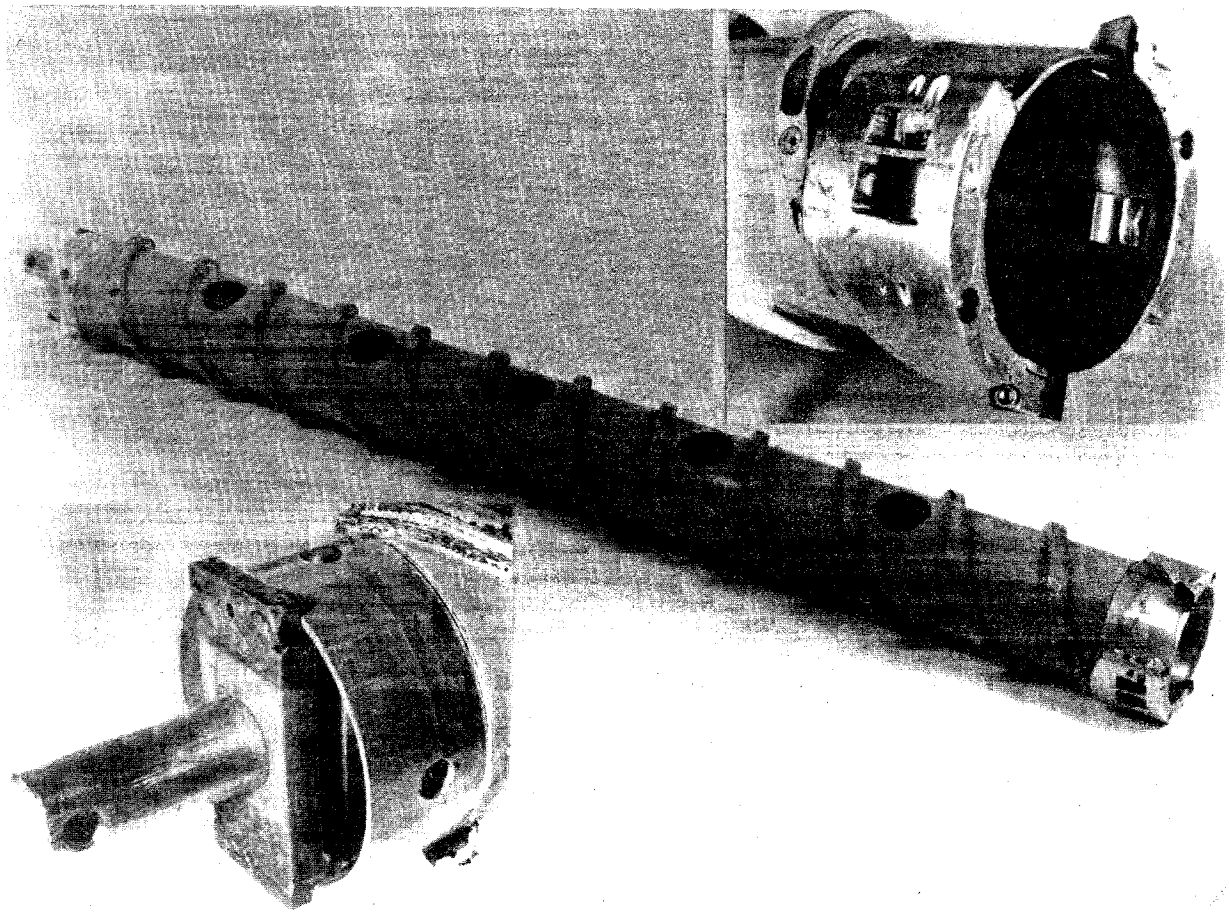

Figure 1. Coring auger used to obtain sea ice samples.

(In prep.). The chief attributes of the core barrel are: very light weight; rapid penetration with low torque and low thrust; high core quality and long lengths of unbroken core; and freedom from jamming problems. Core was commonly retrieved in unbroken lengths up to 1 m with a core diameter of approximately 4.2 in. (107 mm).

The 4.25-in.-diameter coring drill was used mainly for vertical drilling, but it was also used in a horizontal mode for boring into vertical ice walls exposed in excavated pits, or into near-vertical ice walls produced by the natural splitting of multi-year ice ridges.

As core was extracted, it was logged. For each section of core the depth of origin was recorded, and ice temperature was measured immediately after the core was brought to the surface. The core was then sawed into convenient lengths for shipment and final sample preparation. Offcuts of ice were used to provide salinity specimens. These specimens were melted, and electrical conductivity was measured, together with water temperature, in order to determine the ice salinity. Further salinity measurements were made in the testing laboratory after completion of each mechanical test.

Trimmed and logged specimens were packed inside cardboard tubes, each 1.02 m long and 0.108 m diameter inside. The tubes were packed into shipping boxes measuring 1.09×0.38×0.38 m inside. Each box held a maximum of nine tubes, or six tubes when packed with dry ice and snow. After the ice had been transported to Prudhoe Bay in unheated helicopters, dry ice was added to the shipping crates for the first stage of transport to Hanover, New Hampshire. The crates were first flown to Anchorage, where they were put into temporary storage in a refrigerated warehouse until the complete consignment supply was assembled. The crates were then flown to Boston in a single consignment, and were finally carried to Hanover by a refrigerated truck, which met the incoming flight. Final storage was in a CRREL coldroom maintained at a temperature of -30°C. During drilling, logging, handling and shipping, care was taken to minimize contamination, brine loss, mechanical damage, and undue thermal disturbances. Details of the field sampling program are given by Cox et al. (1984).

Specimen preparation in the laboratory

The various steps in the preparation and testing of specimens were carried out at different temperatures, e.g. storage at -30°C, sawing at -10°C, machining at -20°C, testing at up to -5°C. In transferring specimens from one ambient temperature to another, care was taken to avoid thermal shock. Specimens were protected by insulated containers during transfer, and they were allowed to equilibrate with the new environment gradually.

Test material was selected in the storage room by referring to the field log, and the required section of core was carried in its cardboard tube to an ice preparation shop where band saws are located (-10°C). A band saw (Sears 112-23770) was used to rough-cut cylinders to a length of 27 cm (10.6 in.). The most satisfactory blade was 0.5 in. wide with 10 teeth/in. A speed of 3000 ft/min was used to cut the ice. These cylinders were cut from core sections that appeared to be free from gross surface flaws. During the 1981 drilling program some cores were gouged longitudinally by slippage of the core-catcher dogs. Most of the core damaged in this way was discarded in the field, but gouges caused some material to be rejected at the rough-sawing stage. The sawing operation was done in such a way that offcut discs were obtained from both ends of each selected cylinder. These discs were used subsequently for structural analyses (Fig. 2).

Rough-cut cylinders were taken from the saw room (-10°C) to the ice machining room (-20°C). The first step in machining was trimming the ends on the milling machine (Jet JFM-830). The rough-cut ice cylinder was laid horizontally in a cylinder holder, which maintained the axis of the specimen parallel to the surface of the table of the milling machine (Fig. 3). The end surfaces of the ice cylinder were then shaved by a 1-in.-diameter four-flute endmill rotating at 1850 rev/min and traversing across the face at 21 in./min (9 mm/s). The first pass took off 0.050 in., while the final three passes took off 0.005, 0.002 and 0.001 in., respectively. After milling, the ice cylinder was 10.000 ± 0.003 in. (254.00 ± 0.08 mm) long, and the end surfaces were expected to be normal to the axis of symmetry to within 10^{-3} radians (0.06°). The surface of each plane was intended to be flat to within 0.0005 in. (0.013 mm). In principle, departure from parallelism between the end planes could be twice the angular tolerance for squareness of the ends, i.e. up to 0.002 radians (0.11°).

At this stage the specimen diameter was measured at several cross sections by a vernier caliper, the length was measured, and the ice was weighed on a Mettler balance to a resolution of 0.1 g. This permitted the bulk density of the specimen to be calculated.

The end planes were checked for flatness and parallelism by standing the cylinder on the base of

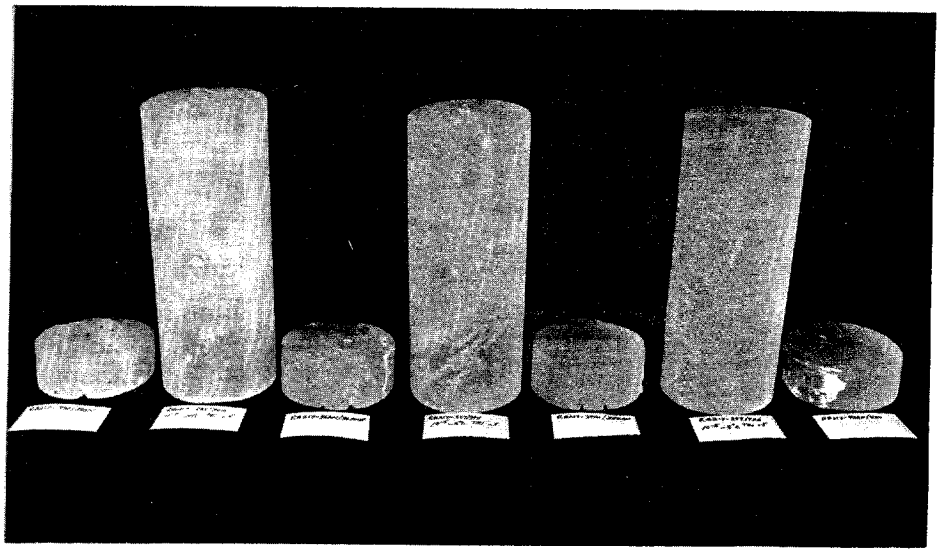

Figure 2. Rough-cut test samples and offcuts for petrographic analyses.

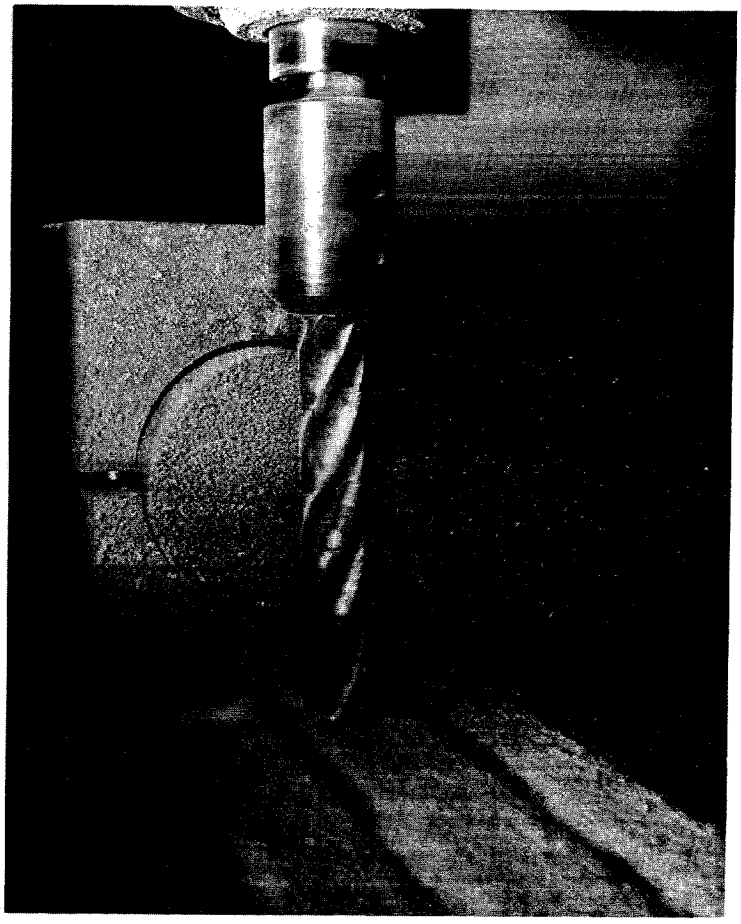

Figure 3. Milling machine trimming ends of rough-cut ice cylinders.

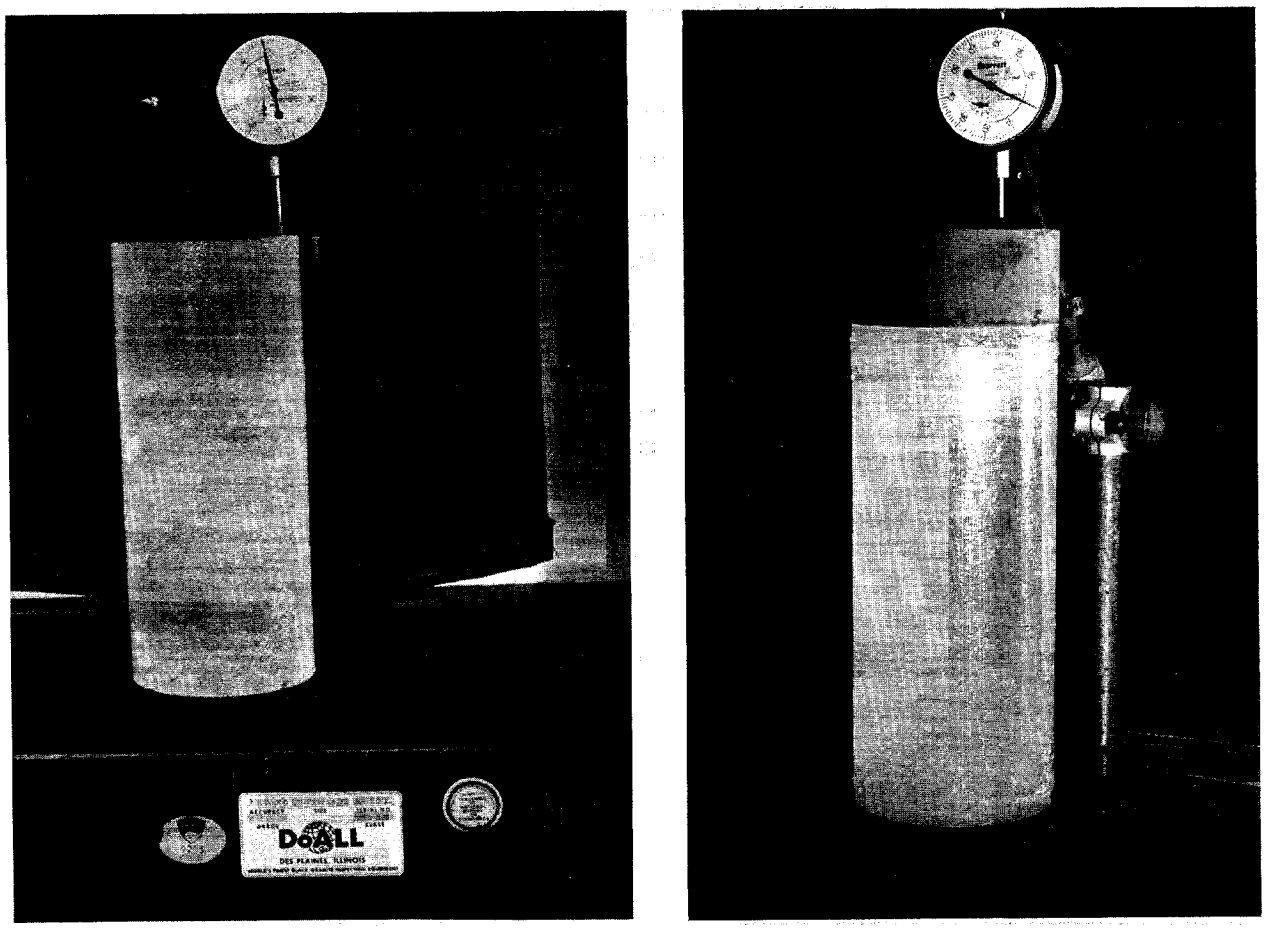

Figure 4. Comparator used for checking the flatness and parallelism of specimen end planes (a) and the parallelism of bonded end caps (b).

a comparator (Fig. 4a) and traversing a dial micrometer over the top end plane. The cylinder was inverted to check the other surface.

The next stage in preparation involved the bonding of end caps to the ice cylinder. These end caps were short cylinders, 4.203 in. (106.8 mm) in diameter by 1.00 in. (50.8 mm) long (Fig. 5). They were made from a phenolic resin reinforced by linen fabric (Synthane, bonded Bakelite, Micarta). The bond face of each end cap was roughened to expose fine linen fibers, and it was deeply incised by a set of concentric grooves. This type of surface was intended to provide high surface area and a strong bond with the ice; the machining technique for producing the surface is described in Appendix A.* Each end cap was also drilled axially from the other (smooth) end, and the hole was tapped with a 1 in.x14 threaded steel rod, penetrating to a depth of at least 1.5 in. (38.1 mm). During manufacturing and subsequent handling, the incised surfaces of the end caps were protected against contamination by oils or other substances that might inhibit bonding. They were also cleaned periodically in acetone.

During the bonding process the ice cylinder and the end caps were aligned in a split-cylinder Lucite jig (Fig. 6). The jig was 13 in. (330 mm) long, and the internal diameter was 4.206 in. (106.8 mm). This gave a clearance of 0.003 in. (0.076 mm) between the end caps and the jig. The clearance between the ice cylinder and the wall of the jig was slightly greater and variable, depending on the diameter of core, which at this stage was still the diameter produced by the field coring drill.

Prior to the bonding operation the incised surfaces of the end caps were soaked in a bath of ice water in a room at 0°C. To start the operation the alignment jig was placed vertically with one cap set in the lower end of the cylinder, the wetted incised surface facing up. A layer of ice water was then spread over the incised surface with a syringe to a thickness of approximately 0.125 in. (3.0 mm). The volume of water was standardized by the syringe.

*Further developments are in progress.

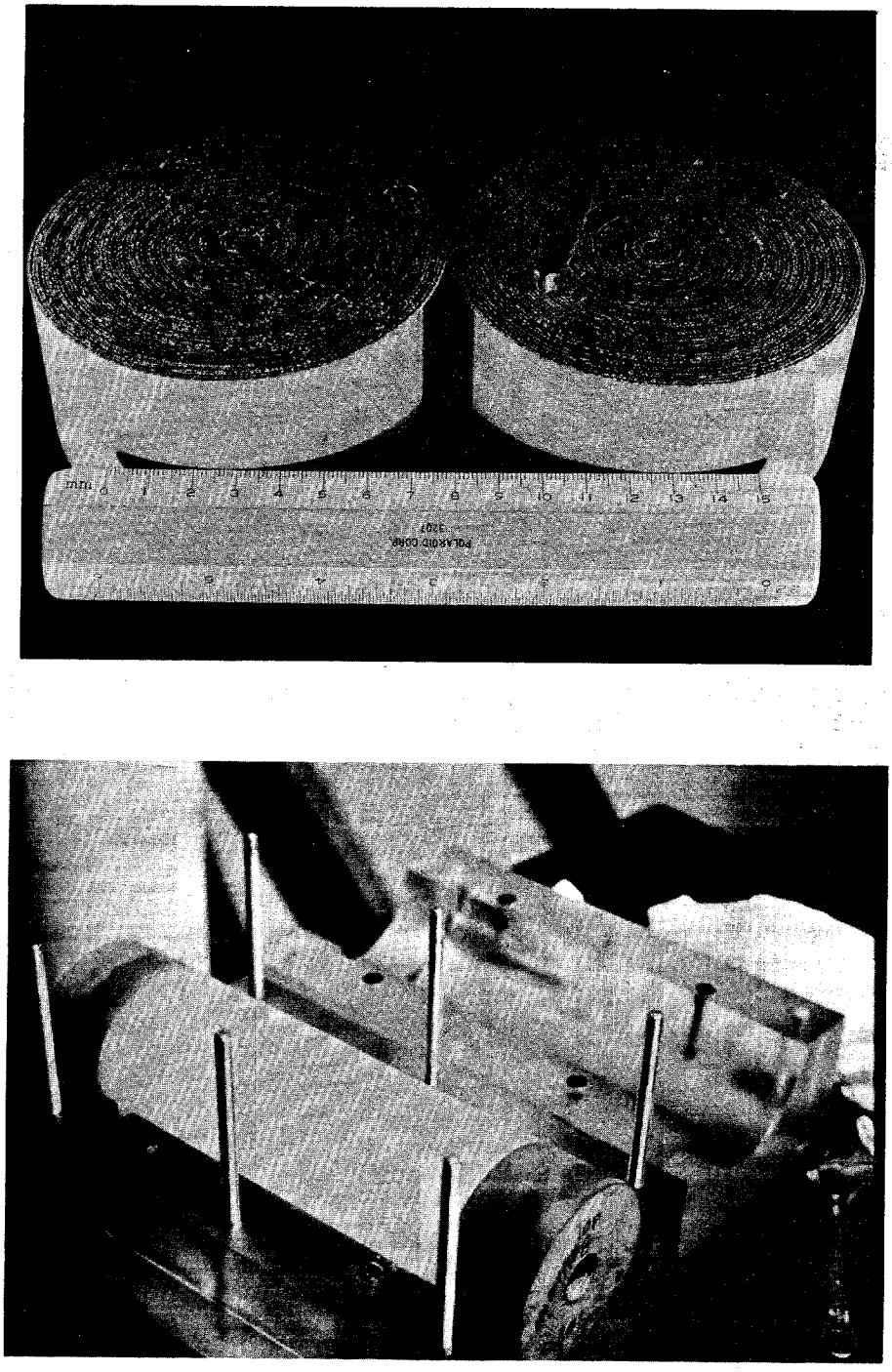

Figure 6. Split-cylinder jig used to align end caps on specimen.

All of this took place at an ambient temperature of 0°C. The cold ice cylinder (-20°C)* was then brought to the jig and was inserted quickly until it came into contact with the cap. Excess water tended to extrude into the clearance annulus. After five minutes the bond was well established, the jig was taken apart, and the specimen was removed. The process was then repeated for the remaining cap and the other end of the specimen. The specimen with both caps fitted was allowed to remain in the room at 0°C for 15 minutes before being returned to the machining room.

The final stage of preparation involved shaping and finishing the cylindrical surface. The specimen

*Higher ice temperatures were used for bonding tensile specimens.

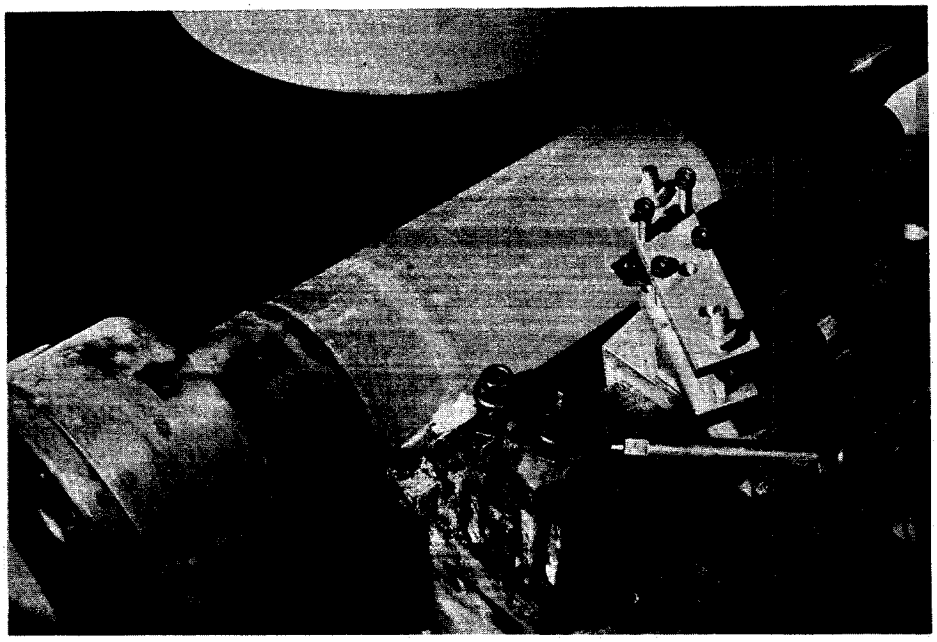

Figure 7. Turning specimen to finished diameter on lathe.

was returned to -20°C temperature and mounted in a lathe (Jet JET-1236P) by gripping one end cap in a three-jaw chuck and by centering a 1 in.x14 threaded rod, screwed into the other end cap, against a live center in the tailstock (Fig. 7). Cutting was done by a specially made form tool with a radius of 8 in. (i.e. twice the specimen diameter). The form tool was set on the tool post with its cutting edge horizontal and at the height of the lathe axis. The radial depth of cut was adjusted in increments, starting with a coarse cut (0.025 in.) and finishing with very shallow cuts (0.003-0.001 in.). The specimen was rotated at 240 rev/min. With the depth of cut set, the form tool was traversed along the length of the cylinder at a rate of 4.75 in./min, the traverse terminating at each end when the form tool was almost contacting the end cap. In this way a long-radius fillet was formed at the transitions from the ice midsection to the end caps. Specimens for compression tests were turned to a diameter of 4.000-0.003 in. (101.60 mm). Specimens for uniaxial tensile tests were turned to a dumbbell shape, with a neck diameter of 3.500-0.003 in. (88.90 mm). The form tool used on the tensile specimens had a radius of 7 in., which was twice the diameter of the finished neck.

Before the specimen was tested, the diameter was remeasured with a dial-type vernier caliper, and the end surfaces of the phenolic caps were checked for parallelism on the comparator (Fig. 4b). The principal axis of tilt was marked so that steel shim stock could be used to compensate for any departure from parallel. Each specimen was also photographed against back lighting to provide a record of gross structure, pores or other inherent characteristics.

APPLICATION OF FORCES AND DISPLACEMENTS TO UNIAXIAL SPECIMENS

Compression

In a uniaxial compression test the objective is to create a uniaxial state of stress in the test specimen, and to maintain that stress state over a range of displacements, or strains.

The first problem is to create a uniaxial stress state by loading a cylinder axially, since there is no known way of applying hydrostatic pressure to the end planes without some kind of circumferential confinement. The traditional method has involved direct contact between flat steel platens and the test specimen. This usually produces radial restraint of the specimen end planes by interfacial friction. The resulting triaxial stress state near the ends of the specimen has been defined by many theoretical and experimental studies [see Hawkes and Mellor (1970) for a summary]. There is a further problem if the surfaces of the specimen and the platens are not perfectly flat. Tiny humps or irregularities create high, but localized, contact stresses, and under conditions which favor brittle fracture these contact stresses can nucleate and propagate cracks long before the bulk

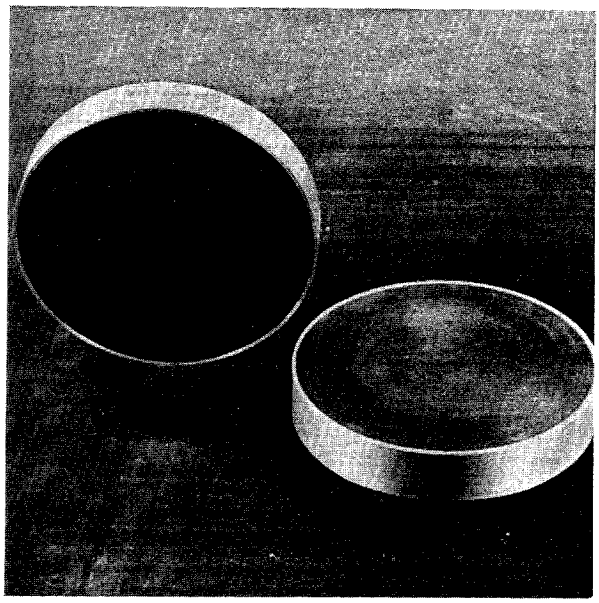

Figure 8. Compliant platens tested in initial stage of project.

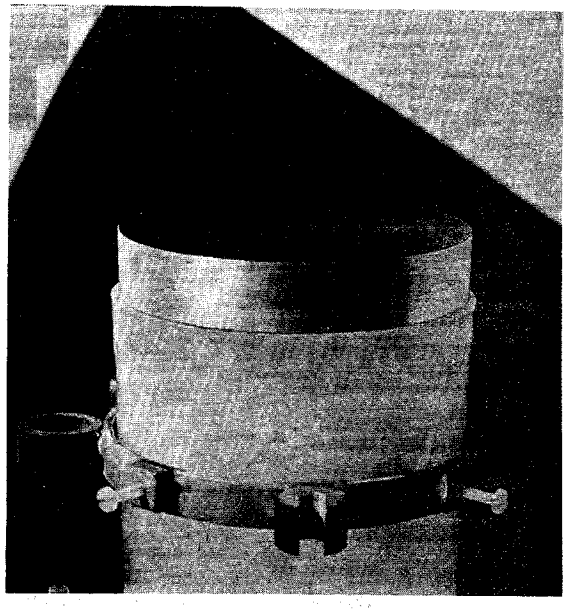

Figure 9. Effect of large radial strains when using compliant platens.

of the material is ready to fail. It might seem that the problems of radial restraint and contact stresses could be solved by placing a layer of soft elastic or plastic material between the platen and the specimen, but while this deals with contact stresses it simply reverses the direction of radial restraint, producing radial tensile tractions at the end planes. If interface "cushions" are to be used to control contact stresses, the best compromise seems to be a thin layer of crushable material, such as paper, which compensates for very small surface irregularities without providing much relief from radial friction. When radial restraints are accepted as an unavoidable condition, the specimen is proportioned so that its center section (which ought to fail first) is essentially free from the end-effect stress field perturbations.

There are ways of greatly reducing radial restraint of the specimen end planes in compression. One way is to use brush platens, such as those employed by Hausler (1981). A brush platen consists of a cluster of slender metal columns arranged with close but precise spacing. Each column has a square cross section; so far brush platens have been made in a square shape for application to prismatic specimens. One objection to brush platens is that the contact stresses are necessarily higher than the mean stress, and there must be stress concentration at the edges of each column (the columns are, in effect, closely spaced punches).

Another way to reduce radial restraint while virtually eliminating contact stresses is to use compliant platens. These were developed for measurement of strength under field conditions where specimens cannot be machined with high precision and where short lengths of core might have to be tested (Haynes and Mellor 1977). The original compliant platens for ice consisted of a plug of elastic urethane confined inside a thick-walled aluminum ring. The internal diameter of the aluminum ring was slightly greater than the unstrained diameter of the ice specimen, the actual annular clearance being designed on the basis of estimated radial strain at failure. The idea was to produce a pressure distribution close to hydrostatic in the urethane while restricting radial strains. Extrusion at the annular clearance space was limited by a judicious choice of modulus for the urethane (less, but not much less, than that of ice).

The original compliant platens met their design goal, but they were never intended for use in high-quality laboratory tests, where they would introduce an undesirable "soft" link in a system intended to be "stiff." Nevertheless, consideration was given to the development of improved compliant platens in this study. The general idea was to reduce the annular clearance between the confining ring and the specimen to zero, and to design a very thin ring that would permit the urethane disk to expand radially at the same rate as the ice specimen. Design calculations (Appendix B) showed that the required ring was too thin to be made with in-house facilities, and at the planned limit of strain for the ice ($\approx 5\%$) an aluminum ring would have passed its elastic limit. A compromise was struck by making platens that were 0.75 in. (19.1 mm) thick, with a urethane disk 4.0 in.

(101.6 mm) in diameter and an aluminum confining ring whose wall thickness was 0.06 in. (1.6 mm). The platen surfaces were faced-off in a lathe so that the confining ring was flush with the urethane surface (Fig. 8). These platens were not satisfactory. The ice expanded more than the platen, and the ice appeared to slip on the urethane. At large axial strains the end of the ice specimen had a greater diameter than the platen, the aluminum ring created stress concentrations, and the platen acted as a punch, causing failure in the vicinity of the end planes (Fig. 9).

A similar problem arose when ground stainless steel platens were used in direct contact with the ice. These platens had a diameter of 4.125 in. (105 mm), and the ice appeared to slide against the steel. In ice tests at Exxon Production Research, Houston, large-diameter steel platens were used, but circular grooves were machined in the steel to prevent excessive radial expansion of the ice.*

Another approach, called platen matching, has been tried in the field of rock mechanics. Platens are turned to the same diameter as the specimen, and the platen material is selected to give a close match of radial strains in the specimen and the platen. The requirement is that Young's modulus E and Poisson's ratio ν for the platen (subscript p) and specimen (subscript s) should be related by:

$$\frac{E_p}{\nu_p} \approx \frac{E_s}{\nu_s} .$$

For metals that might be suitable as platen materials, E/ν might be in the range 2×10^7 to 10×10^7 lbf/in.^{2} (140 to 700 GPa), whereas for typical rocks E/ν might be in the range 0.4×10^7 to 4×10^7 lbf/in.^{2} (30 to 300 GPa). For ice, E/ν is likely to be less than 0.5×10^7 lbf/in.^{2} (35 GPa), so that ordinary metals are out of the question for platen matching. However, plastics such as Lucite or plexiglass might be possibilities.

It was finally decided that, for this testing program, bonded end caps similar to those used by Mellor and Cole (1982) offered the best compromise. The end caps, made of linen-based phenolic resin, are described in the preceding section and Appendix A. Bonded end caps appeared to offer the following advantages:

1) Interfacial contact stresses are eliminated.
2) Interface closure during loading does not occur.
3) Complete radial restraint is guaranteed, even in tests carried to large strains.
4) Specimen preparation on the lathe is simplified (special machining grips are not required).
5) Displacement transducers can be mounted firmly on the end caps.
6) Precise positioning and attachment on the testing machine is facilitated.
7) The same basic preparation technique can be used for both compression and tension specimens.

After the platen problem has been solved, the next consideration in a compression test is control of the motions to ensure that there is precise axial travel, with no flexure or racking of the specimens. In the past, most testing machines had a spherical seat that allowed the upper platen to rotate in order to compensate for lack of parallelism between the specimen end planes. In many cases, spherical seats were designed in such a way that rotation was accompanied by lateral movement [see Hawkes and Mellor (1970) for analysis], and high-pressure lubricants allowed the seat to rotate, even under high loads. This is unacceptable, as any transient departure from symmetry in the internal deformation processes inevitably leads to flexure of the specimen, and hence to premature failure. Another problem arises if the ends of the specimen are able to move relative to each other in horizontal planes, producing racking of the specimen. This type of motion permits the development of unrepresentative slip planes, or shear planes, in the specimen. Although the frame and cross members of a high-capacity testing machine are likely to be very resistant to racking, a long column of attachments (actuator extension rod, load cell, specimen connectors) may have very little flexural rigidity.

For this program no spherical seats were used. The specimen was centered precisely on the axis of the testing machine actuator by means of a locator pin, which protruded from the lower platen. The upper platen, which had no spherical seat, was brought just to the point of contact with the top end cap, the contact was checked with a feeler gauge, and an appropriate piece of steel shim stock was inserted to fill any gap. Early validation tests made with dual axial displacement transducers showed this procedure to be very important. Without perfect parallelism between the machine platen and the specimen end cap, initial loading forced the end cap to rotate slightly, giving initial axial strain rates in the specimen that differed on opposite sides of the cylinder by as much as a factor of two.

Because of the way the environmental cabinet was mounted in the testing machine, there was a long slender column (including a load cell) connecting the top platen to the machine crosshead. This column did not have high flexural rigidity. Further-

*Personal communication with J. Poplin.

more, there was no positive connection between the top platen and the top surface of the upper specimen end cap. This permitted some lateral slip if inclined planes of weakness in the specimen favored gross diagonal shearing during the deformation. Thus, the requirement for prevention of lateral platen translation was not fully met, and a few tests were affected adversely; the results from these tests were discarded.

Tension

Ideally a uniaxial tensile test should be the same as a uniaxial compressive test with the direction of displacement and the sign of the stress reversed. This is possible if dumbbell specimens with bonded end caps are used for both tests, but direct tension tests on simple right-circular cylinders are far from ideal, because stress perturbation near the end planes causes failure to occur there and not in the section where stress is uniaxial.

The first problem in tension testing is how to attach the ice to the pulling device. A variety of mechanical grips and bonding systems have been tried in the past, with varying degrees of success (Hawkes and Mellor 1972, Schwarz et al. 1981). The problem was re-examined at CRREL in 1979, and the possibility of making tests on simple right-circular cylinders was considered. The bonded aluminum caps used by Hawkes and Mellor (1972) and Haynes (1978) were judged unsuitable because differential thermal strains can cause debonding when the temperature is varied over wide ranges. The mechanical grips used by Dykins (1970) are applicable to dumbbell specimens but not to simple cylinders. In the field of rock mechanics, epoxy bonding of simple butt joints has been used with some success, and a comparable arrangement was sought for ice. To deal with the dual problems of low bond strength (especially near 0°C) and stress field perturbation, Mellor proposed the use of bonded end caps with bristles of metal, plastic or organic material projecting into the ice. At that time there were no funds to pursue the idea systematically, but one of the compromise versions of the idea, involving disks of carpet fabric, was used in a simplified form by Currier (1981). Leaving aside the thought of internal reinforcement of the ice, consideration was given to increasing bond strength by roughening the surfaces of plain end caps. A technique for etching the surface of aluminum, proposed by E.M. Schulson,* was apparently unsatisfactory, but scarified surfaces on linen-based phenolic resin gave a good bond. The technique is outlined in Schwarz et al. (1981), and

*Personal communication, Thayer School of Engineering, Dartmouth College, Hanover, New Hampshire.

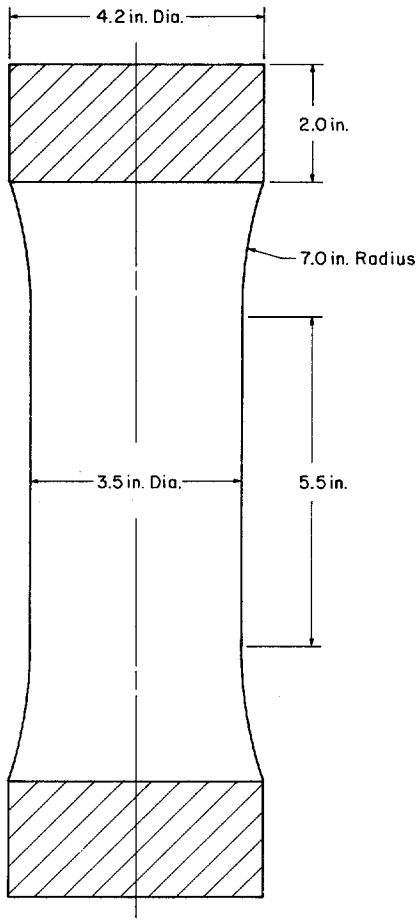

Figure 10. Geometry of tensile specimen.

full details of the standardized machining procedure are given in Appendix A. The use of scarified phenolic end caps was adopted for both tension and compression tests, but events proved that simple cylinders did not provide reliable measurements of tensile strength.

Bonded end caps proved to be very convenient for final machining of both tensile and compression specimens. The standard compression specimen actually had a dumbbell shape after trimming with a form tool from 4.2 in. to 4.0 in. diameter. The difference in cross-section area between the end planes and the central section was only 9% for this specimen. For tensile tests a 9% difference in nominal axial stress was judged to be insufficient to compensate for the combined effects of end-plane stress perturbation, differential thermal strain between the ice and the end cap, and possible large flaws near the end planes. Bond strength tests indicated that dumbbell specimens with a neck diameter of 3.5 in., i.e. cross-section reduction of 31%, would guarantee tensile fracture in the central section. The final geometry of the tensile specimen is shown in Figure 10.

The choice of a long fillet radius was judged to be important, since the stress concentration factor (SCF) for the transition zone is controlled by the fillet geometry. Earlier studies (Hawkes and Mellor 1970, 1972) showed that stress concentration at the transition could be reduced to the 3% level by taking a fillet radius $R_F \approx 2D$, where D is the specimen neck diameter. Increasing R_F provided only slow improvement (SCF = 1.02 with $R_F = 8D$), but decreasing R_F caused significant deterioration (SCF = 1.05 with $R_F = 1.4D$). The actual fillet radius was 7 in., giving $R_F = 2D$ for the tension specimens.

During preliminary testing it was found that tensile specimens that were bonded to the end caps with the sea ice at -20°C were likely to break near the interface instead of breaking in the gauge section. This problem was more or less eliminated when bonds were formed with the sea ice at -15°C, but an ice temperature of -10°C was finally used for routine bonding. It would have been desirable to form the bonds with the sea ice closer to 0°C, but such high ice temperatures could lead to loss or migration of brine in the saline ice.

The end caps of the tension specimen were attached to the testing machine by threaded steel rods screwed into the tapped holes of the phenolic caps. The threads were designed to have ample shear strength to resist the highest tensile forces, assuming that the rods were screwed in to a depth of 1.5 in. or more. Although it was considered desirable to prohibit rotation of the end caps during a test, it seemed necessary to have a connecting link that would have enough rotational freedom to compensate for slight imperfections in end-plane parallelism. A special spherical seat was designed and built, and it was intended to be lubricated with very light mineral oil or kerosene to give some chance of lock-up after initial load application. Because of time limitations this device was not built into the system. Instead, a pair of universal joints already in use by Currier (1981) were employed. Each of these joints had a pin and ball arrangement, which gave complete freedom in flexure and axial rotation.

Squareness imperfections

The specimens were machined so that the end planes met close tolerances for squareness (10^{-3} rad, or 0.004 in. over the diameter). However, the phenolic end caps did not necessarily maintain perfect contact or axiality during the bonding process. The final values for squareness of the bonded end caps are indicated by the histogram in Figure 11, which shows the distribution of departures from squareness

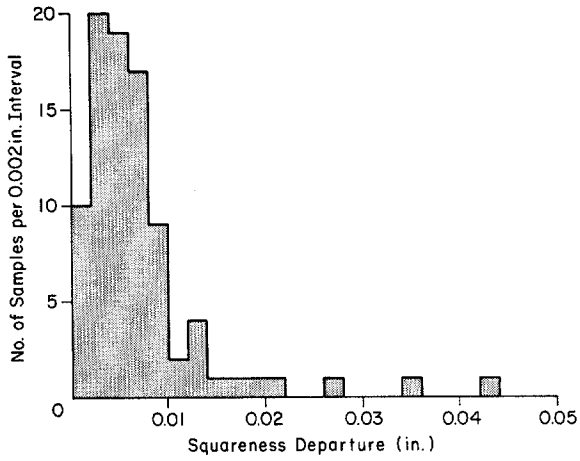

Figure 11. Frequency histogram for departures from perfect squareness of specimen ends.

in the first 80 specimens tested in compression. The modal value for squareness departure is in the 0.002–0.004 in. class interval, and a majority of the samples (85%) had departures less than 0.010 in. Since some specimens failed to meet the selected tolerance for squareness, shimming was used to compensate for lack of parallelism between the faulty end cap and the surface of the platen on the testing machine. Steel shimstock of the required gauge was placed over the "low spot" of the end cap, giving a final contact between the platen and the cap that was close to perfect.

To check whether the shimming technique was effective in removing adverse effects of squareness departures, measured uniaxial compressive strength was plotted against the squareness departure of the capped specimen. Figure 12 gives the results for tests at strain rates of 10^{-3} and 10^{-5}/s, with a test temperature of -5°C. Both plots show considerable scatter, as is to be expected because of the high variability in ice type. However, there are no clear trends, and the linear regression correlation coefficients are 0.19 and 0.08 for 10^{-3} and 10^{-5}/s tests, respectively. Corresponding values of the correlation coefficient at the 95% confidence limit are ± 0.35 and ± 0.34, giving no reason to believe that the correlation coefficients are significantly different from zero. On the basis of this information, it appears that shimming is effective in compensating for small departures from squareness.

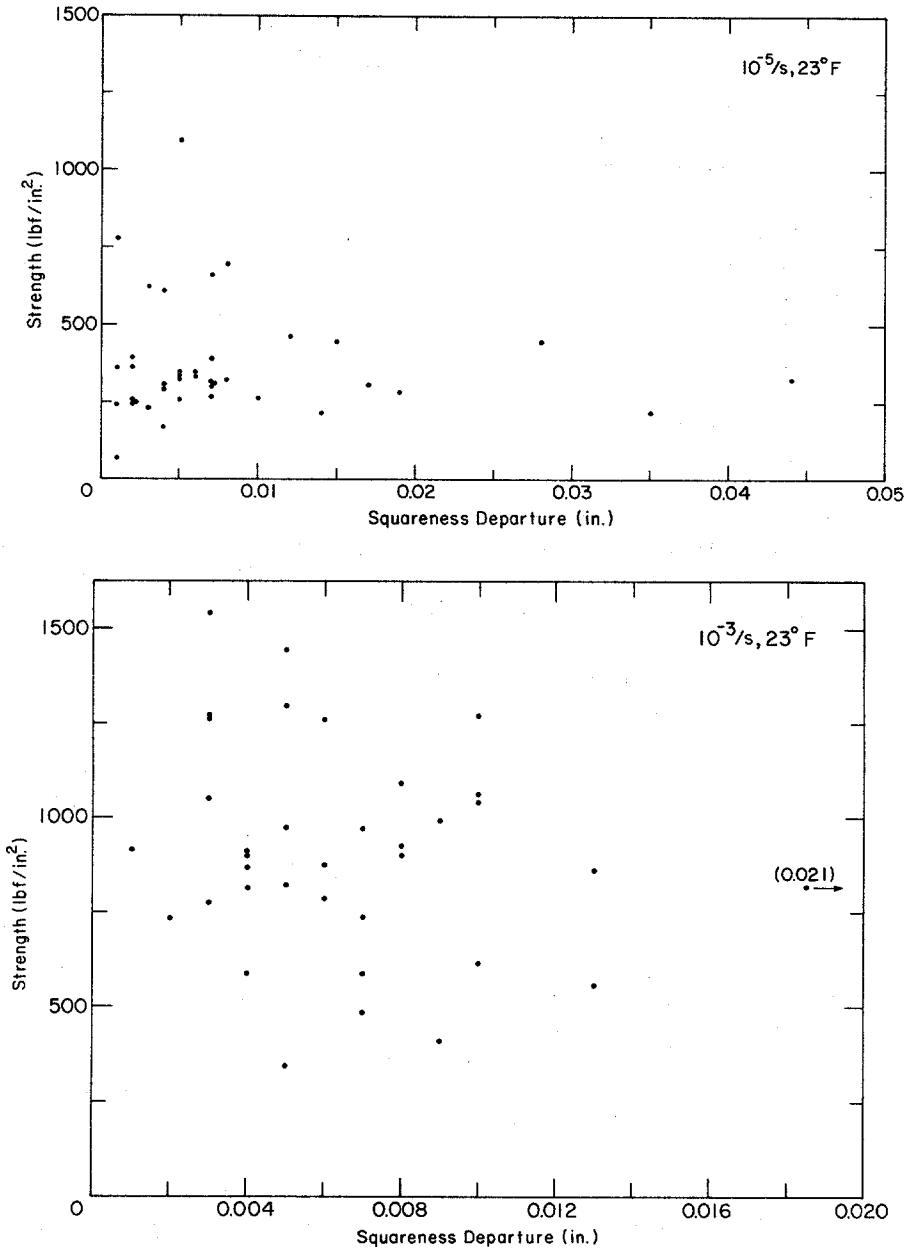

Figure 12. Measured uniaxial compressive strength plotted against squareness departure for tests at -5°C (23°F), with strain rates of 10^{-5}/s and 10^{-3}/s.

LOADING DEVICES

Universal testing machine

The main loading device for this program was a universal testing machine (Fig. 13). The machine was custom built from stock components by MTS Inc. to meet design specifications drawn up by CRREL. One of the major original requirements was for a machine capable of making closely controlled tests on strong materials (such as rocks) and on large specimens (such as frozen gravel specimens). Thus there was a need for high force capability, high inherent stiffness, and rapid response from the closed-loop electrohydraulic system. For this reason the machine has a main frame with a rated working capacity of 500,000 lbf (2.2 MN), and a main hydraulic actuator with a quasi-static force capability of 250,000 lbf (1.1 MN). The servo valve for the main actuator is rated at 90-gal./min flow capacity; it has a 1-kHz frequency response, a 2-3 ms time lag behind the command signal, and it can reach a flow rate of 35 gal./min in 2 ms. The maximum controlled travel speed of the main actuator is 100 in./min

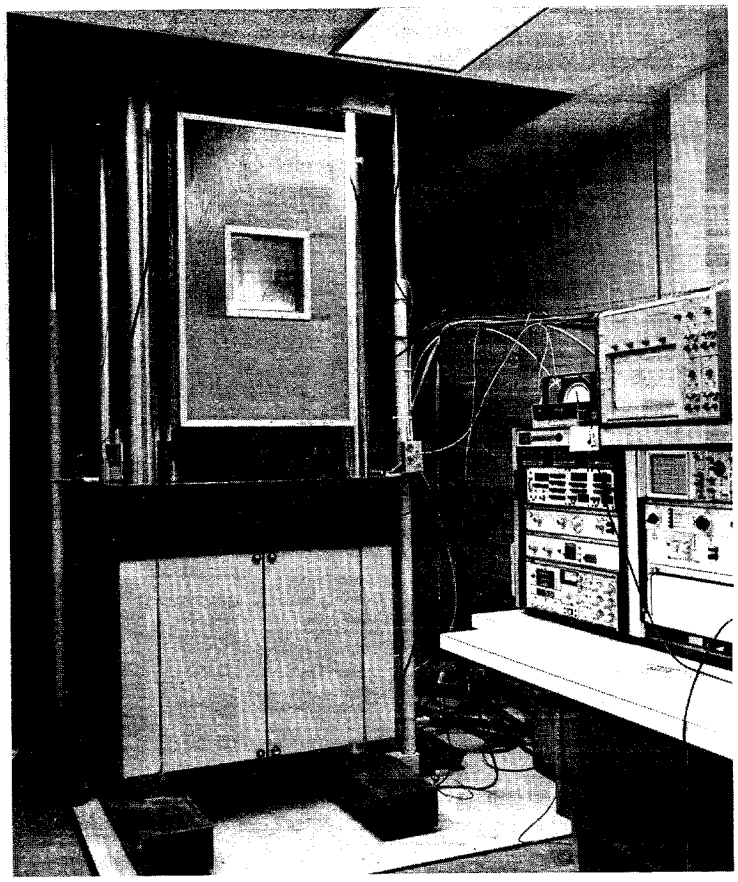

a. Main frame and insulated cabinet.

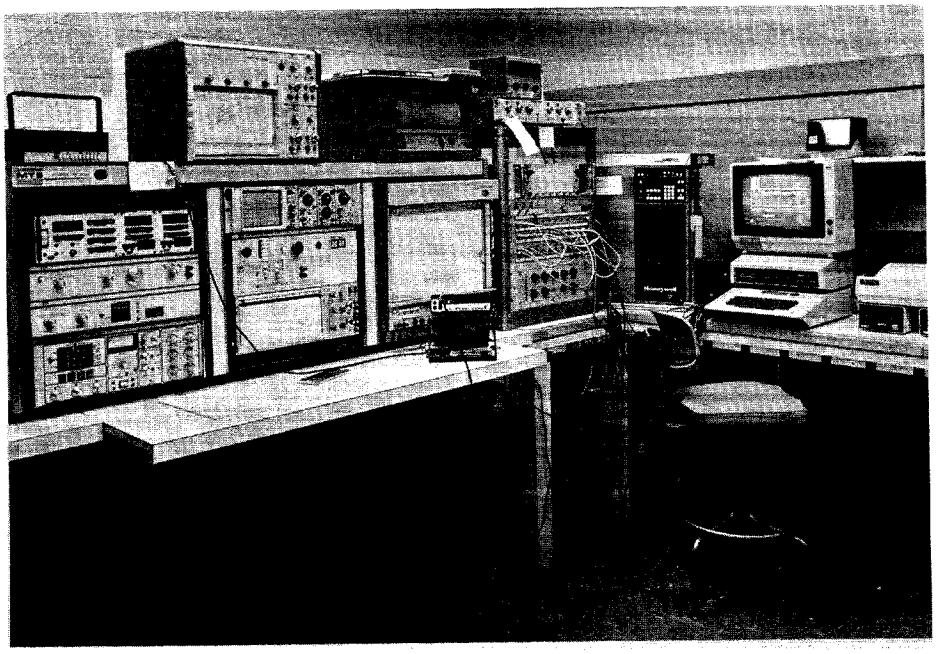

b. Control console.

Figure 13. Universal testing machine.

(42 mm/s). The machine also has a much smaller actuator, which is capable of controlled travel speeds up to 1000 in./min (0.42 m/s) with the high-capacity servo valve. The small actuator has a quasi-static force capacity of 25,000 lbf (0.11 MN), and it is usually controlled through a 15 gal./min servo valve. The main actuator is mounted in the base of the machine, and the small actuator is fitted to a movable cross head. Hydraulic power for the actuators is provided by an electrically driven pump in an adjacent soundproof room.

The universal testing machine can be programmed to control force or actuator displacement as any given function of time. It has integral sensors for force and displacement, but the closed-loop system can also be controlled from external load cells or displacement transducers.

The testing machine is housed at room temperature in an air-conditioned laboratory. The test environment is provided by a refrigerated cabinet set between the columns of the machine frame, and supplemental refrigeration is used to cool the massive lower platen, which penetrates the cabinet. The original cabinet was a commercially built unit providing interior space 20 in. wide by 22 in. high by 30 in. deep (508x559x762 mm). Cold air was supplied through ducts from an independent refrigerator, which was eventually discarded because of unsatisfactory performance and maintenance difficulties. A new supply of cold air was improvised by using the CRREL central refrigeration system and a finely controlled heater. A second insulated cabinet was also built to provide greater interior space, being 20.5 in. wide by 39.5 in. high by 35.5 in. deep (521x1003x902 mm). The final system gave temperatures that were constant within 0.2°C, with a cycle time of minutes.

Gas actuator for constant load

Although the universal testing machine is capable of maintaining a constant force over long time periods, it is too complicated and expensive to be used routinely for constant-stress creep tests of long duration. For constant-load compression tests, two sets of a simple apparatus were built by CRREL. The device was a larger version of an apparatus used for creep tests on 2-in.-diameter ice cylinders by Mellor and Cole (1982). In the original design the specimen was centered in a reaction frame and was compressed axially by an upper platen whose thrust rod was guided axially in a precise linear ball bushing. To save time a simpler design was used for this project (Fig. 14a), but it was not completely satisfactory, and modification to the Mellor and Cole (1982) design (Fig. 14b) is planned. Force was applied by a gas actuator (Bellofram) with a piston area of 24

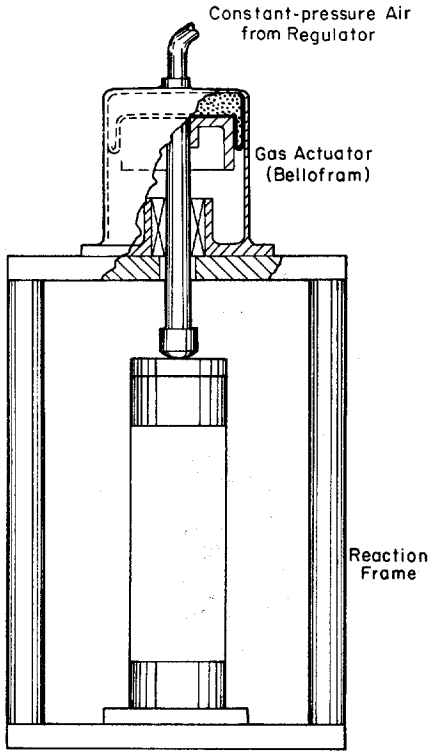

a. Apparatus used for this project.

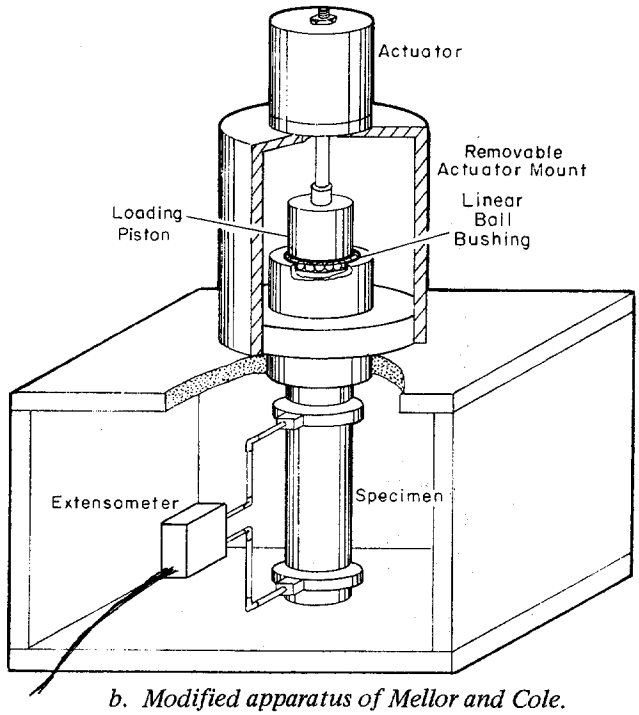

b. Modified apparatus of Mellor and Cole.

Figure 14. Constant-load compression devices.

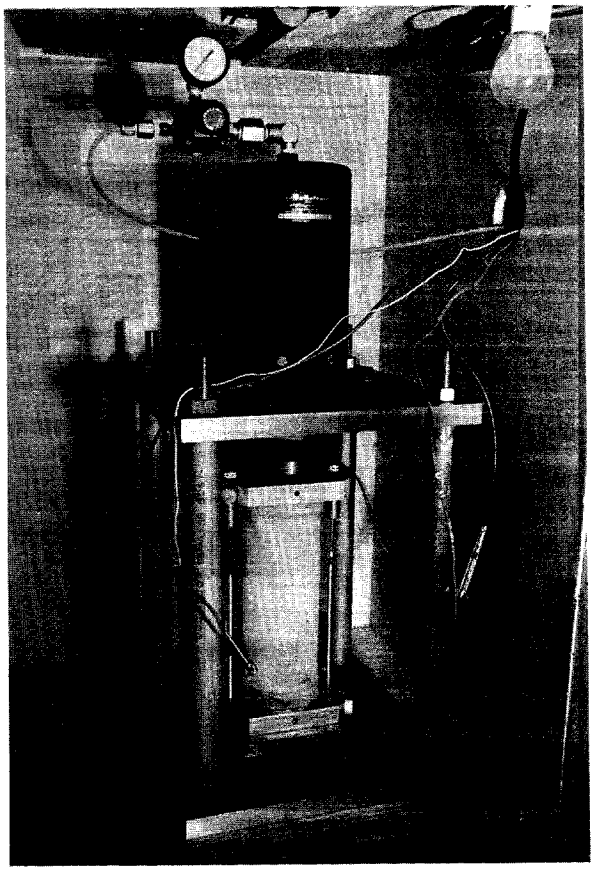

Figure 15. Specimen mounted for compression under constant load.

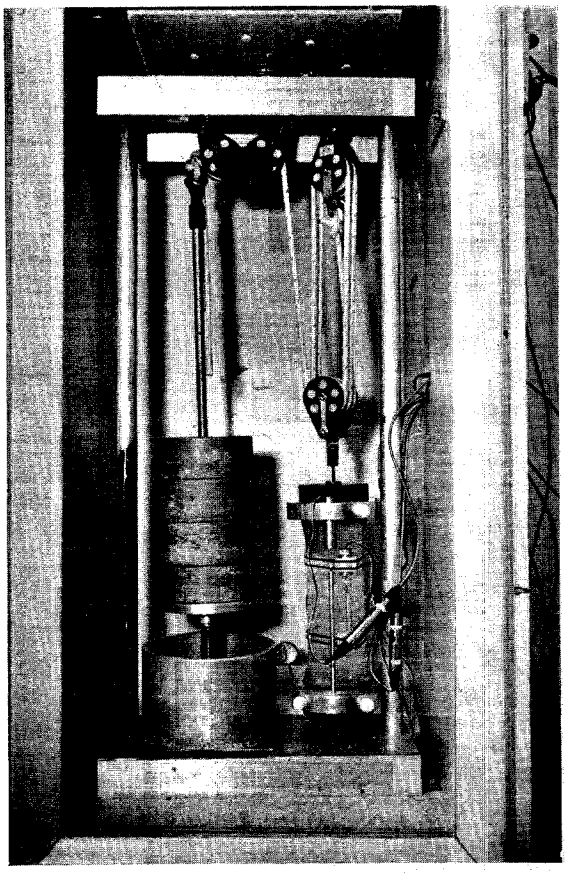

Figure 16. Specimen mounted for tension under constant load.

in.^{2} and a maximum working pressure of 145 lbf/in.^{2} The actuator was pressurized from the laboratory compressed air supply, using a regulator (Bellofram Type 10B) to maintain constant pressure. Set-point pressure was given by a pressure transducer, and the complete unit was calibrated against an electrical resistance strain-gauge load cell. The apparatus is shown in Figure 15.

The constant-load device was kept inside a temperature control box, which itself was inside a walk-in coldroom whose temperature was regulated within course limits. The box was fitted with an air circulation fan, a light-bulb heater, and a temperature regulator. Set-point temperature was adjusted to within 0.5°C of the desired test temperature by trial and error, and once the test was established and stabilized, temperature fluctuations were less than ± 0.5°C (typically ± 0.2°C), with a cycle time of minutes.

Weight-and-pulley system for constant tension

For Phase II of the project a simple device for tensile creep tests was built. The test specimen was attached to a reaction frame, and tension was applied by a system of weights and pulleys (Fig. 16). The device was designed to apply working loads up to about 1000 lbf (about 0.5 kN), using sheaves that multiplied the force of the lead deadweight by an apparent factor of six. The pulleys were yacht sheet blocks rated for a force of 2250 lbf (10 kN). A triple block with a swivel shackle pulled on the top end cap of the specimen through a short flexible connector (steel cable). The upper pulley was a double block with a becket. The weight hanger was connected to the pulleys by halyard line, with two single swivel blocks, each on a deck plate, to guide the first turn. These single swivel blocks were joined by a bracket to maintain separation and alignment. The lower end cap of the test specimen was attached to the base of the reaction frame by a short flexible connector. Each lead weight was approximately 26 lb (12 kg), and each was numbered and weighed individually. The weight system was calibrated by replacing the specimen with a load cell. This accounted for the weight of the lead and the hanger, friction in the pulleys, and lack of perfect parallelism in the lines. The calibration (Fig. 17) showed that the force

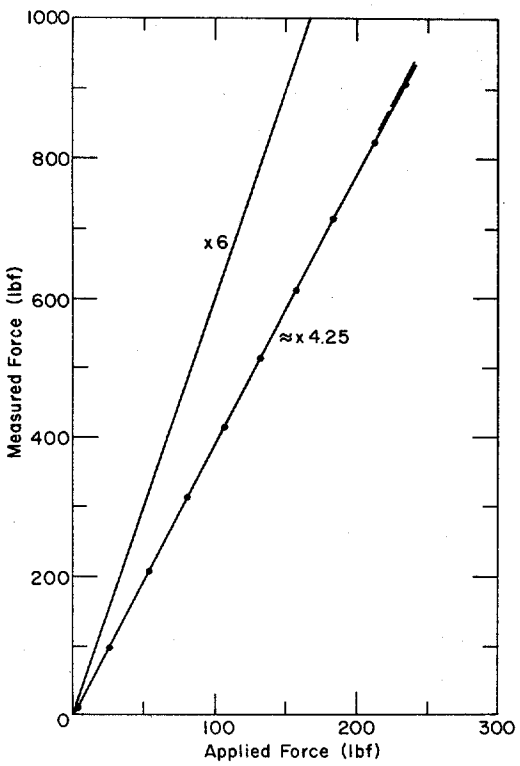

Figure 17. Calibration for the constant-load tension device.

multiplication was approximately 4.25 instead of 6; i.e. the friction was about 1.75 times the applied load. There was a slight tendency for the friction factor to increase with the total load. Prior to testing, the weight hanger was supported on a screw jack. To start a test the screw jack was lowered gradually so as to apply stress to the specimen at a modest rate.

The whole apparatus was housed in a temperature-control cabinet, which itself was inside a walk-in cold-room. Loose snow was placed inside the cabinet to minimize evaporation from the specimen, but this did not completely overcome the problem. For tests of long duration it is preferable to use a membrane or an inert coating on the specimen.

Equipment for triaxial tests

For conventional triaxial compression tests ($\sigma_1 > \sigma_2, \sigma_3; \sigma_2 = \sigma_3$), a special cell was built to accept the capped specimens used for the uniaxial compression tests. The cell itself was an aluminum cylinder with an internal diameter of 5.5 in. (14.0 cm) and a designed working pressure limit of 5000 lbf/in.^{2} (35 MPa). In the final version the upper cap of the cylinder was extended and provided with a bushing to maintain axial stability in the push rod and the pressure-sealed piston (Fig. 18). A novel feature of the triaxial apparatus was a special intercylinder that allowed the axial thrust pressure and confining fluid pressure to maintain the same ratio (σ_3/σ_1 = constant) throughout the test. The complete triaxial apparatus (Fig. 19a) was mounted inside the environmental cabinet of the universal testing machine (Fig. 19b), where it was loaded by the main actuator of the machine. The intercylinder that maintained the ratio provided a fixed value for that ratio. To change the ratio it was necessary to change the piston area of the intercylinder, either by inserting a sleeve and a new piston, or by using a completely different intercylinder. Fluid pressure was measured by a pressure transducer, and external force was measured by a load cell. The piston seals had very low friction.

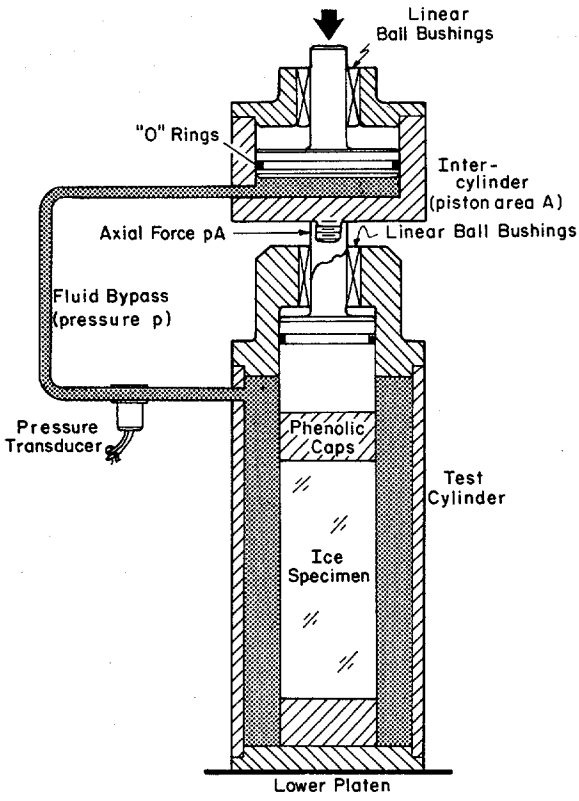

Figure 18. Diagram of the triaxial compression test equipment.

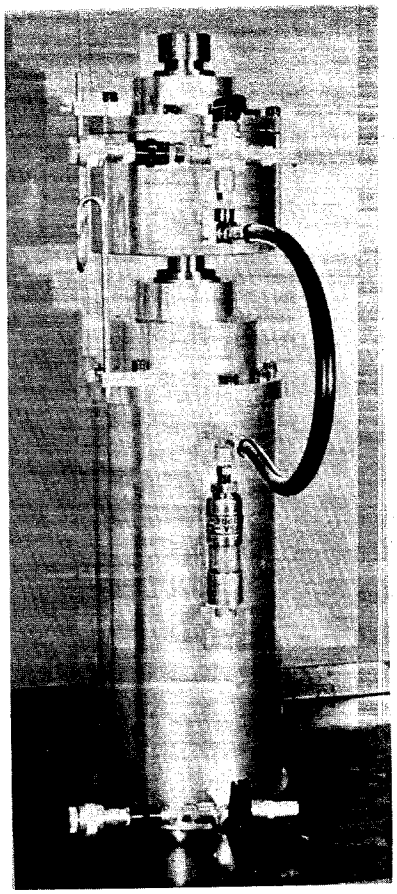

a. Triaxial apparatus.

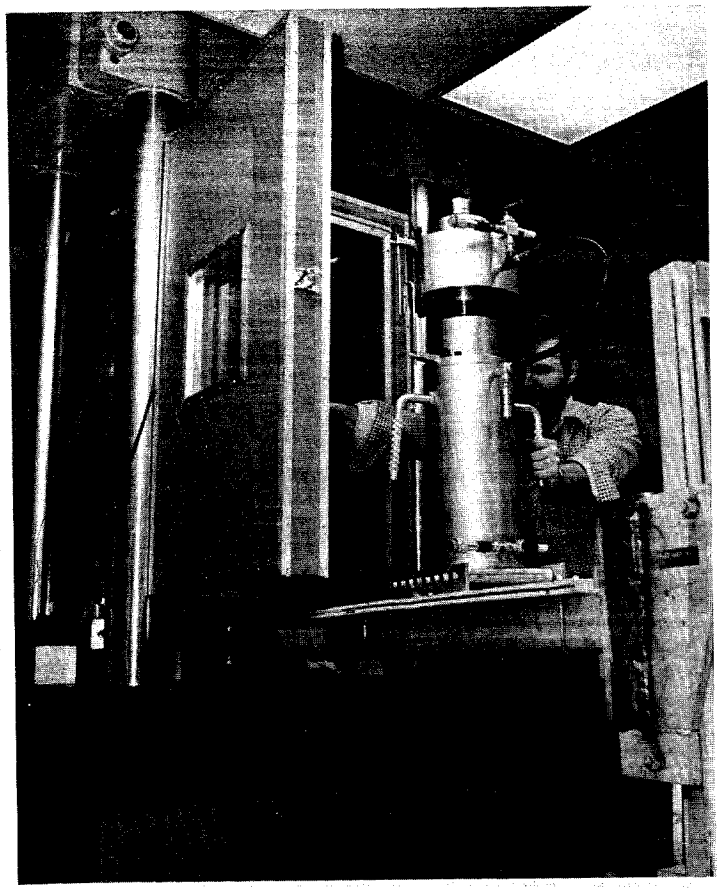

b. Apparatus being loaded into environmental cabinet.

Figure 19. Pressure cell for conventional triaxial tests, with an intercylinder to provide a constant σ_1/σ_3 stress ratio.

MEASUREMENT OF FORCE AND DISPLACEMENT

Force

The integral force-measuring system of the testing machine, which is based on a pressure transducer in the hydraulic fluid, was not used as a primary force-measuring device for normal testing. Instead an electrical-resistance strain-gauge load cell (BLH) was attached above the upper platen. A cell with a 50,000-lbf capacity was selected for the compression tests, in which loads ranged up to 27,000 lbf. This gave readings well within the acceptable range for the cell (> 10% of capacity) without sacrificing much stiffness in the load cell element of the general test system. Because of time constraints the same cell was used for the relatively few tensile tests of Phase I, but in subsequent tensile tests a smaller cell will be used. The same cell was also used for triaxial tests, in which the applied axial force went to the limit of the load cell capacity during some tests. A larger cell will be used for future triaxial tests. The load cell was calibrated about once a month in the CRREL calibration laboratory, using standards that are checked periodically by the National Bureau of Standards.

For triaxial testing the axial force applied to the system by the machine actuator was measured by the load cell described above. With zero friction in the sliding pressure seals of the triaxial cell, this force would equal the axial force on the specimen. With no fluid pressure in the triaxial cell, friction in the seals and guides is negligible, but the system has not yet been checked under pressure. With zero friction in the sliding seals of the intercylinder, fluid pressure in that cylinder, and in the triaxial cell, would be the externally applied axial force, as measured by the load cell, divided by the piston area. The actual fluid pressure was measured by a pressure transducer, and comparison of these readings with

calculated pressures for both forward and reverse piston motion showed that seal friction was negligible for practical purposes.

Displacement

The testing machine has integral displacement transducers on the actuators, but these do not give a reliable measure of axial displacements within the test specimen itself because of the various connections and interfaces between the machine and the specimen. The original intent was to attach demountable displacement transducers to the midsection of the specimen, using these to give both the test record of axial strain and the feedback signal to the closed-loop control system. However, to control the machine and to maintain a reliable record of displacement up to large specimen strains ($\approx 5\%$), it proved necessary to employ an additional transducer with firm and stable connections to the bonded end caps of the specimen.

The preferred device for measurement of displacement was the DCDT (direct-current displacement transducer), since it has high resolution and is not prone to damage if the specimen shatters. The intent was to use two transducers on opposite sides of the specimen, with wiring to give an average displacement for the two transducers. Measurements were to be made over a gauge length of 5.5 in. (14.0 cm) in the midsection of the compression specimen, where the stress field is not much perturbed by end effects. The brand of DCDT was chosen in response to advice from a colleague,* who examined the precision, stability and temperature response of readily available brands.

In designing the first mounting system for axial DCDTs (Fig. 20), the aim was to have frames that were very light, that minimized stresses and stress concentrations at the attachment points, and that accommodated large radial strains in the specimens. Very light aluminum frames held the DCDTs and their core rods, and each frame was attached to the ice by four spring-loaded pins. Each pin had a sharp point to provide slight penetration of the ice surface, with an adjustable nut limiting the penetration depth. The spring on each pin had a low modulus and long travel. For mounting on the specimen, the two frames were aligned relative to each other by removable rods, and they were positioned on the specimen with the aid of a jig (Fig. 21). This attachment system proved unsatisfactory, largely because the delicate attachments allowed the frames to be disturbed by normal handling, by the electrical signal wires, by machine vibrations, or even by forced air circulation

* Personal communication with R.T. Martin, Massachusetts Institute of Technology, Cambridge, Massachusetts.

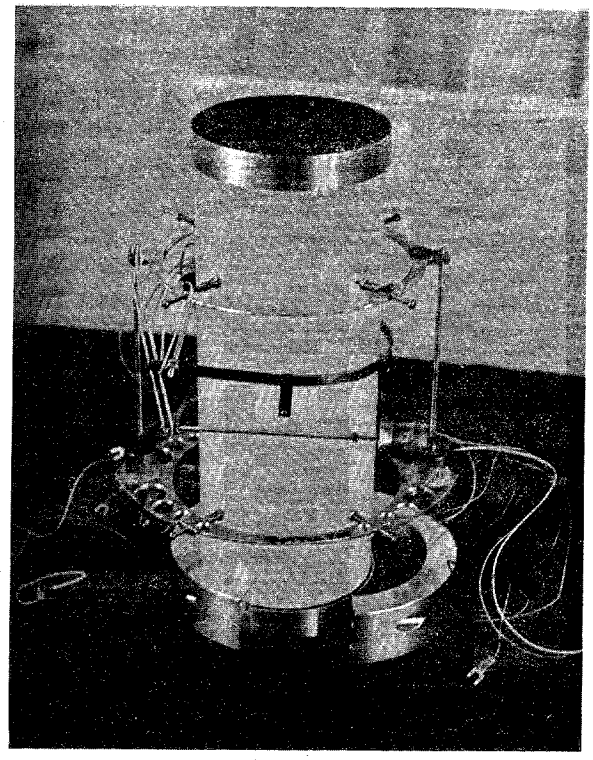

Figure 20. First version of the DCDT mounting system for measuring axial strains. Also shown are two yoke assemblies used to measure radial strains.

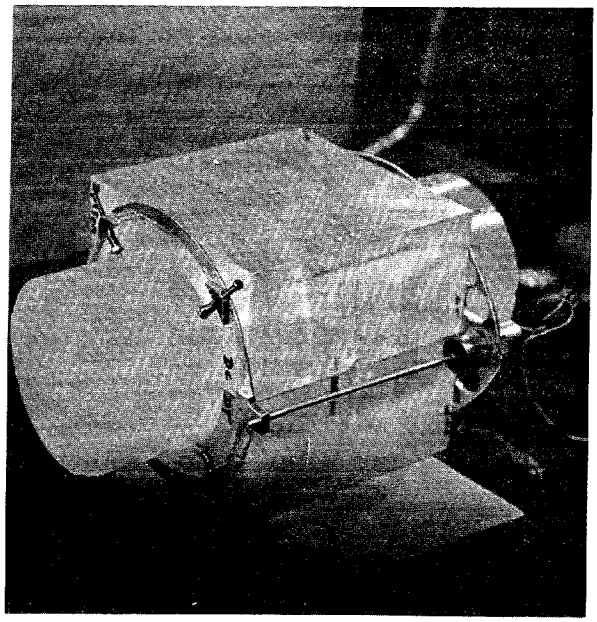

Figure 21. Jig used to position DCDTs and their support frames on ice specimen.

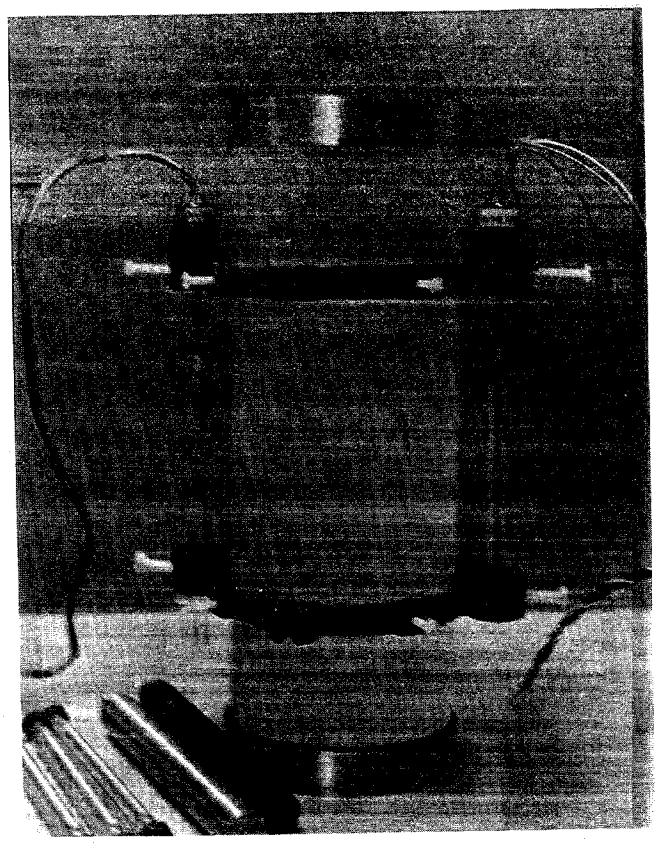

Figure 22. Second version of the DCDT mounting system.

in the environmental cabinet. It was also found that the core rods of the DCDTs tended to bind when irregular deformation of the ice surface caused relative motion or rotation between the two frames. The DCDT used for the project was especially prone to binding because of the very small clearance between the core rod and the transformer (much smaller than the typical clearance of LVDTs).

The aluminum frames were discarded, and a different approach to mounting axial DCDTs was tried. Holders for the transducers and their core rods were cemented to a pair of springy fiberglass rings, which were cut from thin-wall fiberglass tubing (4.25-in. internal diameter). Each ring was clamped to the ice by four Teflon screws (Fig. 22), and it accommodated radial expansion of the ice by deforming elastically. Unlike the previous arrangement there was no rigid connection between the push rods of the lower ring and the core rods of the transducers in the upper ring. The push rods were 0.25-in.-diameter Lucite rods with their end surfaces faced off in a lathe. The core rod of each transducer rested under its own weight on the upper end of the Lucite push rod, so there was no binding when the push rod and the transducer core ceased to be perfectly aligned. Before attachment to the specimen the rings were set to the correct spacing and relative orientation by a pair of removable rods. When tests were run to large strains, the clearance between the mounting rings and the ice proved to be insufficient, causing the screws to bite into the ice and finally allowing contact between the ring and the ice. This problem might have been surmounted by using larger rings, but it was decided to try something more predictable.

In the final scheme each DCDT and each push rod was mounted in a small block of Teflon, which was machined to a radius matching that of the unstrained ice surface (Fig. 23). A pair of DCDT blocks was fastened at opposite ends of a diameter by rubber bands (large O-rings), and the matching pair of push rod blocks was similarly fastened in an appropriate position. Positive location of each Teflon block was assured by a pair of small, sharp pins projecting from the block. The concave contact surface of each block was cut by a set of thin, milled radial slots to permit some deflection of the Teflon in conformance with radial strain of the ice specimen, and also to minimize heat conduction from the DCDT to the ice. As in the previous setup there was no rigid connection between the transducers' core rods and the push rods

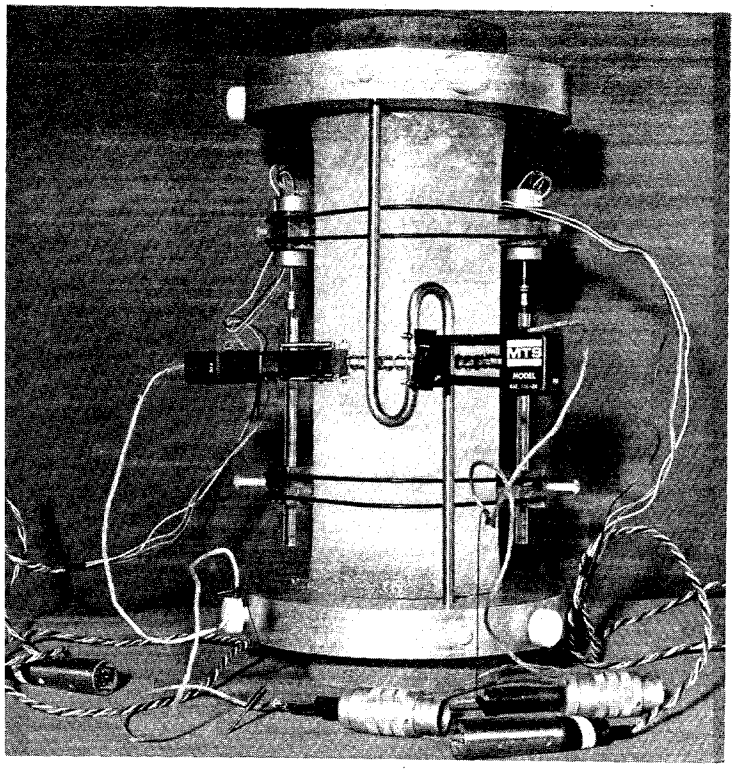

a. Compression specimen with axial DCDTs, axial extensometer and circumferential extensometer.

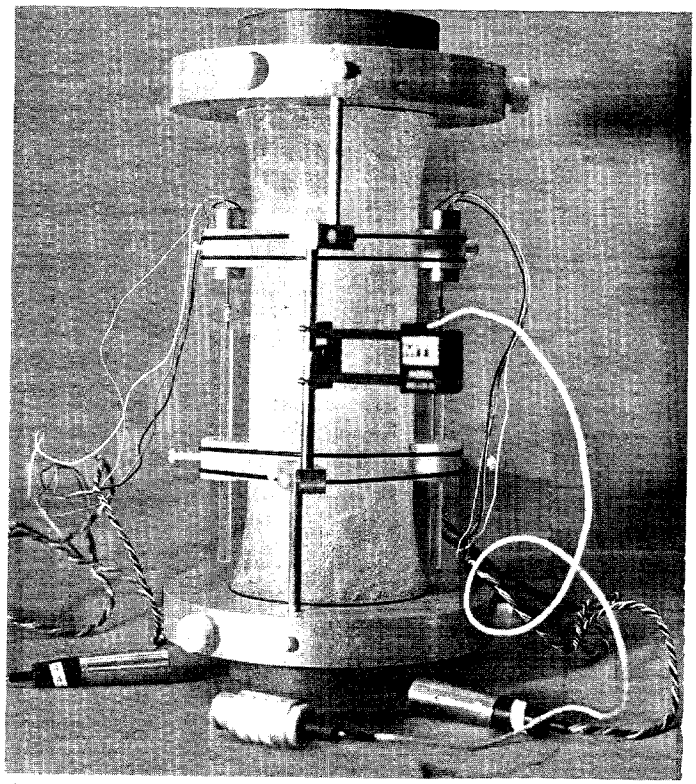

b. Tension specimen with axial DCDTs and axial extensometer.

Figure 23. Scheme finally adopted for measuring strains on test specimens.

of the lower mounts. The Teflon blocks were spaced correctly and aligned relative to each other by removable rods.

The Teflon-block mounting system was judged to be satisfactory for tracking axial strains up to the failure point, but it was obvious that no gauges mounted on the ice, not even bonded strain gauges, were likely to give meaningful records at large strains (3-5%). At these large strains the originally cylindrical specimen may tend to barrel shaped, the ice surface may become lumpy, surface cracks may form, and irregular displacements may occur because of specimen inhomogeneity or anisotropy. Some additional instrumentation seemed necessary to provide stable control signals for the testing machine, and to provide a representative record of axial strains up to 5%.

For machine control and wide-range strain measurements, a single displacement transducer measuring between the bonded end cap was used. This arrangement, which had been used successfully in earlier work on smaller specimens (Mellor and Cole 1982), employed a pair of hooked push rods clamped rigidly to the end caps, together with a strain-gauge extensometer operating in a tensile sense (Fig. 23a). The extensometer was supplied by the maker of the universal testing machine (MTS) for use with that machine. During the early part of each test, simultaneous records were obtained for strain in the specimen midsection (from the extensometer). Comparison of these records permitted evaluation of end effects, which appeared to be very small. At large strains the DCDT system ceased to operate reliably, and the only record of axial strain was that from the extensometer. For tension tests the same system was used, but without the hooked reversal rods for the extensometer (Fig. 23b).

Figure 24 gives a comparison of strain measurements made by DCDTs within the gauge length (GL strain) and corresponding strain measurements made by the extensometer over the full length of the compression specimen (FS strain). The range of the data is from about 0.05% to 0.8% axial strain. Although the data have appreciable scatter, there is an approximate 1:1 correlation. There appears to be a tendency for FS strain to be somewhat greater than GL strain, which is rather surprising if the interface is, in fact, fully bonded.

The original test plan called for measurement of radial strain in two orthogonal directions on the central cross section of the specimen. The purpose of this was to study the effect of anisotropy on Poisson's ratio. To measure displacement across a diameter, a DCDT was attached to a yoke, following a system used earlier on rocks (Hawkes and Mellor 1970). Each yoke (Fig. 20 and 25) was very light in weight, consisting of a U-shaped strip of steel, 1/4 in. by 1/16 in. in cross section. The yoke was attached to the ice by a pair of pivot points, which also served as the measuring contacts. These points were offset from the yoke to provide the necessary clearance for use of two yokes at the same cross section. The DCDT was attached across the open end of the yoke, where the displacement caused by sample expansion at the contact pins was magnified by a lever effect. The off-center weight of the DCDT was supported from above by a long rubber band of low modulus. The yokes were awkward to attach to the specimen, which already had axial displacement transducers fitted. After a number of tests it appeared that orthogonal measurements of diametral strain were more likely to create confusion than understanding, since surface displacements tended to be irregular,

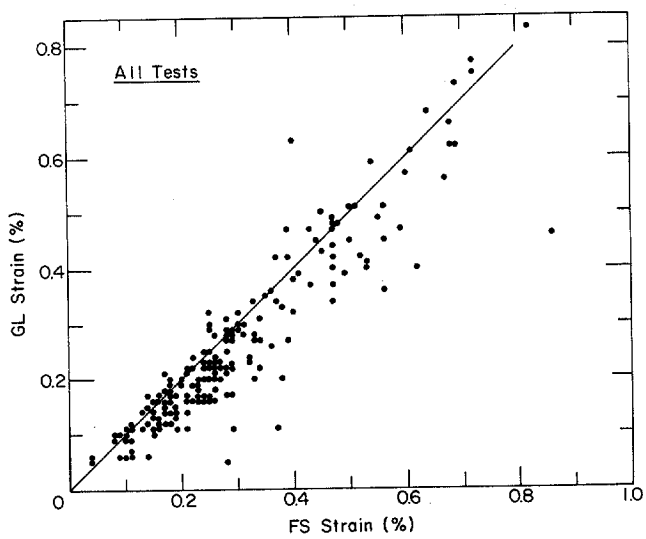

Figure 24. Comparison between full-sample and gauge-length strain measurements.

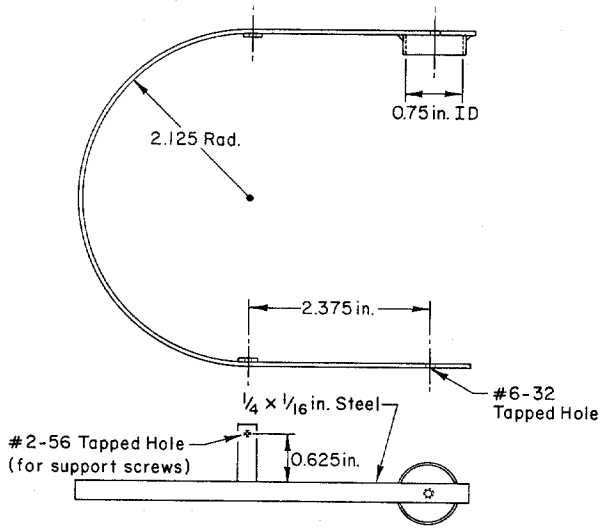

Figure 25. Details of original (MkII) yoke for measuring radial strains.

and petrographic analyses showed that most specimens were inhomogeneous, without any well-defined anisotropy in the horizontal plane. For this reason it was decided that radial strain would be determined from measurements of overall circumferential strain at the midsections. Because of this change in plan a variant of the DCDT yoke based on a scissor mechanism was never tested, although a Lucite prototype was built.

The device finally used for measuring circumferential strain was basically a standard piece of equipment from the manufacturer of the universal testing machine. It consists of a roller chain wrapped around the midsection of the specimen, together with an extensometer used in the extension mode. The only modification required for this project was an extra long chain for the large specimens, and an extensometer with appropriate travel. The device, which did not perform very well, is shown mounted on a specimen in Figure 23a.

During the equipment development phase, two other schemes for measuring radial strain were considered. One involved the use of a pair (or two pairs) of proximity sensors, as used by Cole (1978). Aluminum-foil targets are bonded to the specimen at opposite ends of a diameter, and the proximity sensors are mounted near the targets. Each sensor (Kaman MULTI-VIT) has a coil that induces an eddy current in the foil target, and changes in the impedance of the coil are measured as the separation of coil and target changes. The resolution is 10^{-5} in. One of the objections to this system was that there would be tangential relative motion between the target and the externally mounted sensor due to axial displacement of the specimen. To overcome the general problems of relative axial motion between the specimen midsection and any sensor attached to the testing machine, a special floating mount was designed. The first design used push rods attached to upper and lower platens, with a pivoted cross-linkage whose center remained centered between the platens during platen motion. An improved design used a hydraulic system to maintain an instrument support platform midway between the platens (Fig. 26). This was achieved by having the total axial displacement of the platens divided by a factor of two. Two hydraulic cylinders, with piston areas differing by a factor of two, were connected to give a platform displacement half that of the platens. This device was not built because it would have delayed the start of testing, but the idea appears to have merit. Other arrangements for the same purpose are shown in Appendix D.

For triaxial tests the axial displacement was measured by an extensometer mounted externally between the triaxial cell and its piston. Because the triaxial cell, the piston and the specimen end caps are relatively stiff, and because the specimen is bonded securely to its end caps, this arrangement gives a good approximation for the displacement over the full 10-in. length of the specimen.* Under confining pressure the strain ought to be more uniform along the length of the specimen than it is in a uniaxial state; measurements have shown that the difference between midsection strain and overall strain is very small, even in the uniaxial case (Fig. 24).

It was intended that measurements of both axial strain and circumferential strain should be made on

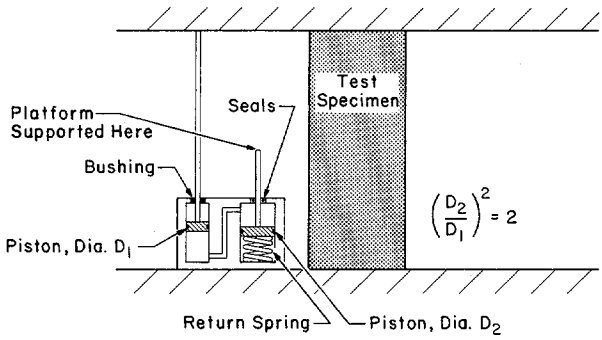

Figure 26. Hydraulic device for supporting an instrument platform at the level of the specimen midplane.

*Recent work has shown that specimen end caps made from phenolic resin are too soft for triaxial testing when axial displacement is measured outside the pressure cell. Aluminum end caps have been substituted. Displacement transducers must also be mounted on the specimen to obtain reliable modulus data.

triaxial specimens by means of bonded constantan strain gauges, so a supply of suitable gauges (4-in. gauge length) was obtained. However, these have not yet been used because of time constraints in the testing program.

In the initial tensile tests under constant strain rate, axial displacement was measured only between the specimen end caps by an extensometer. With a perfect bond between the end caps and the specimen, this displacement divided by the total length of a dumbbell specimen should give an overall strain that is smaller than the strain in the necked section. In earlier work at CRREL (Hawkes and Mellor 1972) this problem was resolved by deriving a calibration factor from simplified theoretical calculations and from strain-gauge measurements on a dummy specimen. More exact theoretical factors for both elastic conditions and creep conditions have since been derived (Appendix C). For this program the intent was to add DCDTs to the necked section of the specimen to give direct measurements of strain in the gauge length (Fig. 23b). Comparison of these strains with overall extensometer readings was expected to provide a calibration factor for the overall apparent strains. For the last four tensile tests of Phase I this procedure was followed, with the surprising result that gauge-length strains turned out to be slightly lower than overall strains. This has not yet been explained, although it is possible that the bond between the ice and the end caps may be tending to yield.

When constant-load tests were made under uniaxial compression in the pneumatic actuator units, axial displacement was measured by a pair of DCDTs mounted between the bonded end caps of each specimen (Fig. 15). In a few trial tests, DCDTs were also mounted on the ice, but since both sets of DCDTs gave the same results, the DCDTs on the sample were eliminated in later tests.

The extensometers and DCDTs were calibrated periodically by applying precise displacements with a special screw micrometer. Calibrations were made for the total system, including the transducer (or transducer pair), the connections and the recorder.

Readouts and recorders

The main output from each test was a record of force and displacement, both as functions of time. For tests that were relatively slow and of long duration (strain rates of the order of 10^{-5}/s), graphical records were obtained directly, using an X-Y plotter (Gould 3054) to give force versus displacement, and two strip chart recorders (a two-channel and a four-channel) to give force and displacement as functions of time. Force and displacement were also recorded in analog form on magnetic tape using an FM recorder. For the tests at relatively high strain rates (10^{-3}/s) the X-Y plotter and one of the strip chart recorders (Gould 110) were too slow to provide reliable records. However, one strip chart recorder (Gould 2400 S) had a 50-Hz frequency response and gave reliable records, while the tape recorder was able to cope with all tests. Analog records from the tapes were subsequently digitized by Shell Development Company in Houston.

For the constant-load compression tests on the pneumatic actuator units, displacement was recorded as a function of time in digital form on paper tapes. The recorder used for these tests was unsatisfactory because of noise and drift, and it will be replaced by a new digital recording system (Hewlett-Packard 3421 A). During constant-load tests, actuator pressure was monitored by a standard pressure gauge on the regulator.

In the triaxial tests the fluid pressure transducer was recorded on the high-speed strip chart recorder and on magnetic tape.

The temperature in the environmental cabinet of the universal testing machine was monitored by a digital bridge, but was not recorded continuously. Temperatures in the enclosures for the constant-load tests were recorded in digital form on paper tape.

LITERATURE CITED

Cole, D.M. (1978) A technique for measuring radial deformation during repeated load triaxial testing. *Canadian Geotechnical Journal,* **15**:426–429.

Cox, G.F.N., J.A. Richter-Menge, W.F. Weeks, M. Mellor and H. Bosworth (1984) Mechanical properties of multi-year sea ice, Phase I: Test results. U.S.A. Cold Regions Research and Engineering Laboratory, CRREL Report 84-9.

Currier, J.H. (1981) The brittle to ductile transition in polycrystalline ice under tension. M.S. thesis, Thayer School of Engineering, Dartmouth College, Hanover, New Hampshire.

Dykins, J.E. (1970) Ice engineering–Tensile properties of sea ice grown in a confined system. Naval Civil Engineering Laboratory, Technical Report R689.

Gradshteyn, I.S. and I.M. Ryzhik (1965) *Table of Integrals, Series, and Products.* New York: Academic Press (translated from Russian).

Hausler, F.U. (1981) Multi-axial compressive strength test on saline ice with brush-type loading platens. *Proceedings of the IAHR International Symposium on Ice, Quebec, Canada, 27–31 July,* Vol. 2, pp. 526–536.

Hawkes, I. and M. Mellor (1970) Uniaxial testing in rock mechanics laboratories. *Engineering Geology*, 4(3):177-285.

Hawkes, I. and M. Mellor (1972) Deformation and fracture of ice under uniaxial stress. *Journal of Glaciology*, 11(61):103-132.

Haynes, F.D. (1978) Effect of temperature on the strength of snow-ice. U.S.A. Cold Regions Research and Engineering Laboratory, CRREL Report 78-27. ADA 067583.

Haynes, F.D. and M. Mellor (1977) Measuring the uniaxial compressive strength of ice. *Journal of Glaciology*, 19(81):213-223.

Jones, S.J. and H.A.M. Chew (1981) On the grain-size dependence of secondary creep. *Journal of Glaciology*, 27(97):517-518.

Mellor, M. and D.M. Cole (1982) Deformation and failure of ice under constant stress or constant strain-rate. *Cold Regions Science and Technology*, 5:201-219.

Mellor, M. and I. Hawkes (1971) Measurement of tensile strength by diametral compression of discs and annuli. *Engineering Geology*, 5:173-225.

Moriguchi, S. and S. Hitotsumatsu (1956) *Mathematical Formulas, Book I: Differentials and Integrals. Plane Curves.* Tokyo: Iwanami Publishing Company (text in Japanese).

Rand, J.H. (In prep.) The CRREL four-inch ice coring auger. U.S.A. Cold Regions Research and Engineering Laboratory, Special Report.

Schwarz, J., R. Frederking, V. Gavrillo, I.G. Petrov, K.I. Hirayama, M. Mellor, P. Tryde and K.D. Vaudrey (1981) Standardized testing methods for measuring mechanical properties of ice. *Cold Regions Science and Technology*, 4:245-253.

APPENDIX A: PHENOLIC-RESIN END CAPS

The phenolic-resin end caps are prepared by first machining the material to the required dimensions. All surfaces of the end cap are smooth, and the flat surfaces are square and parallel to within 0.0005 in. A hole is then drilled and tapped to a depth of 1-½ in. in one end of the end cap to accommodate a 1 in. ×14 threaded steel rod. The rod provides a relatively stiff connection between the specimen and the testing machine. The face of the end cap that is bonded to the ice is then prepared according to the following procedure.

Step 1: The end cap is chucked accurately in the lathe, and the lathe is set up for a spindle speed of 125 rev/min and a feed speed of approximately 4.7 in./min. A special sharp tool with 0° rake, 30° clearance and 15° top angle is set in the tool post with its point parallel to the spindle axis and its cutting tip adjusted vertically to be on center. The tool is set to give an axial cutting depth of 0.010 in. at the center of the cap, the feed is engaged, and the tool makes a spiral traverse across the face of the cap. This produces a "hairy" surface that is incised to a depth of 0.010 in.

Step 2: The next step is to cut a set of circular grooves into the face, using the same special tool. The grooves are spaced 0.100 in. apart, i.e. 200 divisions advance on the perpendicular feed knob of the lathe. The depth of each groove is 0.050 in. (the in-line travel of the toolpost is 0.050 in. from the setting used for the spiral scuffing of Step 1).

Step 3: A wire brush is applied to the face of the cap while it is rotating, so as to remove long shreds of cut material. However, the fine "hairs" should not be removed, as these help in the bonding process. Care should be taken throughout to ensure that the face of the cap is not touched by oil, oily tools or oily hands.

APPENDIX B: COMPLIANT PLATENS

To analyze the plug-ring combination of the compliant platen, assume the following properties:

$$\textit{Aluminum:}\quad E_{al} = 10\times10^{6}\ \text{lbf/in.}^2,\ \nu_{al} = 0.33;$$

$$\textit{Urethane:}\quad E_{u} = 5.5\times10^{3}\ \text{lbf/in.}^2,\ \nu_{u} = 0.30;$$

$$\textit{Ice:}\quad E_{i} = 1.23\times10^{6}\ \text{lbf/in.}^2,\ \nu_{i} = 0.33.$$

The aluminum confining ring is assumed to be filled with urethane over its complete length, and to be pressurized by a radial pressure p. When the plug of urethane is loaded axially by an ice cylinder of the same diameter, the axial stress in both ice and urethane is σ_c. Thus the radial pressure p is

$$p = \frac{\nu_u}{1-\nu_u}\sigma_c = 0.43\ \sigma_c .$$

The radial displacement of the aluminum ring ΔR is

$$\Delta R = \frac{pR^2}{E_{al}t}\left[1 - \frac{\nu_{al}}{2}\right]$$

where R and t are the radius and wall thickness of the ring, respectively.

The radial strain of the ice in its midplane depends on the loading rate, i.e. on the relative magnitudes of elastic and viscous components of strain. For loading at very high rates the pure elastic radial strain ϵ_{re} is

$$\epsilon_{re} = \frac{\Delta R}{R} = \nu_i\frac{\sigma_c}{E_i} = 2.68\times10^{-7}\ \sigma_c .$$

For this case, equality of radial strain in the ice and the ring is given by

$$2.68\times10^{-7}\ \sigma_c = \frac{0.43\ \sigma_c}{10\times10^{6}}\cdot\frac{R}{t}\cdot 0.835.$$

With $R = 2$ in., this gives $t = 0.268$ in.

For practical purposes it is unrealistic to assume purely elastic strain in the ice. In polycrystalline freshwater ice the axial strain at failure is typically on the order of 10^{-2} with mixed-mode rupture at strain rates less than 10^{-4}/s. Since there is some constant-volume flow and some dilatation prior to final failure, we can take $\nu_i \approx 0.5$ for want of a better value. Thus, if the radial strain is 5×10^{-3}, the required wall thickness for the aluminum cylinder is

$$5\times10^{-3} = \frac{0.43\,\sigma_c}{10\times10^6} \cdot \frac{R}{t} \cdot 0.835$$

$$t/R = 7.18\times10^{-6}\,\sigma_c\,.$$

With $\sigma_c \approx 1000$ lbf/in.^{2} and $R = 2$ in., $t = 0.0144$ in. This is about 1/64 in. and probably too small for the simple machining we propose to employ. The strain in the aluminum is also too high for comfort in 60-61 T6 aluminum. An "exact" design can be achieved for ice that fails at small strain, provided that results of pilot tests are available for guidance. However, using a simple elastic ring around a low-modulus plug, it does not seem practical or feasible to have full radial compliance for very high strains. Taking into account the well-documented success of a very simple thick-wall device, we therefore propose to accept a design compromise along the following lines: a) design the aluminum ring to expand to somewhere near its elastic limit, and b) rely on a small radial clearance plus the low shear modulus of the urethane to accommodate further expansion of the ice.

If we use 60-61 T6 aluminum, the elastic limit of strain can be taken as about 3.5×10^{-3}; this value could perhaps be doubled using high-strength aircraft alloy (70-75). The lower value gives

$$3.5\times10^{-3} = \frac{0.43\,\sigma_c}{10\times10^6} \cdot \frac{R}{t} \cdot 0.835$$

$$t/R = 1.03\times10^{-5}\,\sigma_c\,.$$

With $\sigma_c = 1000$ lbf/in.^{2} and $R = 2$ in., $t = 0.0205$ in. This might constitute a very good compromise if special machining can be arranged.

At present the machine shop foreman prefers not to take the wall thickness below 1/16 in. This would allow the platen to strain to

$$\Delta R = \frac{0.43\,\sigma_c}{10\times10^6} \cdot \frac{2}{0.0625} \cdot 0.835 = 1.14\times10^{-6}\,\sigma_c\,.$$

With $\sigma_c = 1000$ lbf/in.^{2}, this is a radial strain of 1.14×10^{-3}. For low-rate tests the radial clearance has to allow for an additional radial strain of about 4×10^{-3}, i.e. an annular clearance width of 0.008 in. As a practical matter we need a clearance on the diameter of about 0.004 in., so this annulus is hardly a matter of great concern.

In the earlier design the urethane plug had a thickness that was 40% of the diameter. For the new platen we would like to limit the plug thickness so as to minimize the compliance, but at the same time the plug has to be thick enough to pressurize the aluminum ring effectively, and any slight bulging into the clearance annulus has to represent only a small fraction of the total volume. The plugs now on order are to be 0.75 in. thick, i.e. 19% of the diameter.

In these calculations no allowance has been made for differential thermal strain between the urethane and the aluminum, although we believe that the expansion coefficient for the urethane exceeds that for aluminum. At a later stage, differential thermal strain can perhaps be utilized to refine the design.

APPENDIX C: THEORETICAL FACTOR FOR CONVERTING OVERALL STRAIN TO GAUGE-LENGTH STRAIN IN DUMBBELL SPECIMENS*

For uniaxial tensile tests on ice and frozen soils it is advisable to use suitably designed dumbbell specimens (Fig. C1). To measure stress-strain characteristics, the strain or displacement should be measured on the neck of the dumbbell, but experimenters sometimes measure axial displacement over the complete specimen length because of difficulties in attaching transducers to the neck. If strain is approximately elastic, a good estimate of strain in the neck ϵ_N can be made from the overall apparent strain ϵ_L, but there is no generally accepted relation for making this estimate. For example, Hawkes and Mellor (1972) made a rough calculation of the required conversion factor, and checked it experimentally by strain-gauge measurements on a dummy specimen made from epoxy resin.

Overall axial displacement ΔL consists of

$$\Delta L = \epsilon_N L_N + 2 \int_0^{\ell} \epsilon_r \, dx \tag{1}$$

where

L_N = neck length (Fig. C1)
ℓ = fillet length
ϵ_r = axial strain where the fillet radius is r
x = axial distance between this section and the end of the neck.

With axial force F on a specimen of neck radius r_N and Young's modulus E

$$\epsilon_N = F/(\pi r_N^2 E) \tag{2}$$

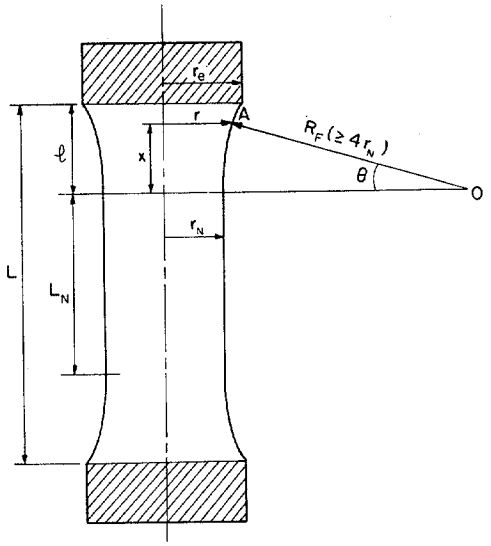

Figure C1. Geometry of dumbbell specimen.

*Also published in *Cold Regions Science and Technology*, 8(1): 75-77,1983.

and

$$\epsilon_r \approx F/(\pi r^2 E)\,. \tag{3}$$

The approximation in eq 3 arises from the fact that $\sigma_{rr} \neq 0$ in the fillet, but it is good approximation because $\sigma_{rr} << \sigma_{xx}$ with realistic specimen geometry. If the fillets of the dumbbell are circular arcs tangential to the neck

$$r = r_N + R_F(1-\cos\theta) \tag{4}$$

in which R_F is the fillet radius and θ is the angle swept by OA as x and r increase from zero and r_N, respectively.

Making substitutions from eq 2, 3, and 4 into eq 1

$$\Delta L = \epsilon_N\left\{L_N + 2R_F \int_o^{\theta_{max}} \frac{\cos\theta}{[1+(R_F/r_N)(1-\cos\theta)]^2}\,d\theta\right\}. \tag{5}$$

The ratio of overall strain ϵ_L to strain in the neck ϵ_N is

$$\frac{\epsilon_L}{\epsilon_N} = \frac{L_N}{L} + \frac{2R_F}{L}\int_o^{\theta_{max}} \frac{\cos\theta}{[1+A(1-\cos\theta)]^2}\,d\theta$$

$$= \frac{r_N}{L}\left\{\frac{L_N}{r_N} + \frac{2A}{(1+2A)}\left[\frac{(1+A)\sin\theta_{max}}{1+A-A\cos\theta_{max}} + \frac{2A}{\sqrt{1+2A}}\tan^{-1}\left(\sqrt{1+2A}\,\tan\frac{\theta_{max}}{2}\right)\right]\right\} \tag{6}$$

where L is the overall specimen length and $A = R_F/r_N$. If the radius of the specimen end planes is r_e

$$\sin\theta_{max} = \ell/R_F \text{ and } \cos\theta_{max} = (R_F - r_e + r_N)/R_F\,. \tag{7}$$

For the specimen geometry favored at CRREL, $A \approx 4$, $L_N/r_N \approx 3$, $\theta_{max} \approx 20°$, $L/r_N \approx 6$. From actual values (Fig. C2) the calculated ratio ϵ_L/ϵ_N is 0.92 for the Hawkes and Mellor (H&M) specimen, and 0.95 for a larger specimen used in these sea ice studies (the CRREL/Shell specimen).

This calculation is not applicable when there is appreciable inelastic strain because of the strong nonlinearity of the stress-strain-rate relation. Furthermore transitions from one creep stage to another may not be synchronous over the whole specimen length. The situation is easy to appreciate by comparing strain rates in the specimen neck and near the fillet ends where $r = r_e$. Assuming a power relation between strain rate $\dot{\epsilon}$ and stress σ such that

$$\dot{\epsilon} = a(b\sigma)^n = a\left(\frac{bF}{\pi r^2}\right)^n \tag{8}$$

where a, b and n are constants, then

$$(\dot{\epsilon}_e/\dot{\epsilon}_N) = (r_N/r_e)^{2n}. \tag{9}$$

If $n = 3.5$, then $(\dot{\epsilon}_e/\dot{\epsilon}_N) = 0.09$ for $(r_N/r_e) \approx 0.71$ (H&M specimen) and $(\dot{\epsilon}_e/\dot{\epsilon}_N) = 0.39$ for $(r_N/r_e) \approx 0.88$ (CRREL/Shell specimen).

For more systematic consideration, displacement rate V between the end caps of a creep specimen can be expressed as

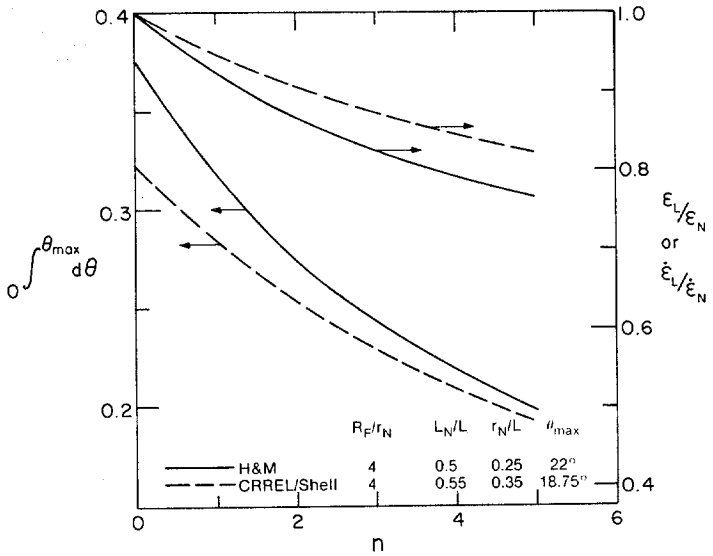

Figure C2. Numerical values of eq 11 as a function of n for two sets of specimen dimensions. Values of the integral in eq 12 are also shown.

$$V = \dot{\epsilon}_N \left(L_N + 2R_F \int_0^{\theta_{max}} \frac{\cos\theta \, d\theta}{[1+(R_F/r_N)(1-\cos\theta)]^{2n}} \right) \tag{10}$$

so that the ratio of overall strain rate $\dot{\epsilon}_L$ to strain rate in the neck $\dot{\epsilon}_N$ is

$$\frac{\dot{\epsilon}_L}{\dot{\epsilon}_N} = \frac{1}{L} L_N + 2R_F \int_0^{\theta_{max}} \frac{\cos\theta \, d\theta}{[1+A(1-\cos\theta)]^{2n}} . \tag{11}$$

The integral is listed (e.g. Gradshteyn and Ryzhik 1965, p. 148, Mariguchi and Hitotsumatsu 1956, p. 190):

$$\int = \frac{1}{(2n-1)(1+2A)} \left(\frac{(1+A)\sin\theta}{[1+A(1-\cos\theta)]^{2n-1}} + \int \frac{(2n-1)A \, d\theta}{[1+A(1-\cos\theta]^{2n-1}} \right.$$

$$\left. + (2n-2)(1+A) \int \frac{\cos\theta \, d\theta}{[1+A(1-\cos\theta)]^{2n-1}} \right) \tag{12}$$

which is too tedious to evaluate. Fortunately some pocket calculators can now do the required numerical integration directly. Figure C2 shows the values of the integral and the values of $\dot{\epsilon}_L/\dot{\epsilon}_N$ for a range of values of n. Numerical values for the H&M specimen and for the CRREL/Shell specimen are used. With $n = 3.5$ as a representative value for high-stress creep tests, strain measurements made between the end caps could be in error by 15-20%, depending on the specimen proportions.

In all of this it is assumed that there is perfect bonding between the ice and the end connectors, and that there are no significant perturbations of strain or strain rate near the interface. These assumptions may not always be justified. For the H&M specimen, mismatch of thermal strain between the ice and the aluminum end cap can lead to slip at very low temperatures (i.e. far from the bonding temperature). For the CRREL/Shell specimen, stress at the bonded interface is relatively high, and some localized yielding is possible.

To sum up, measurement on the specimen neck is obviously desirable, but if this is not feasible, a correction factor can be calculated. With perfect bonding, error in the correction factor is a second-order effect, and adjusted strain values should be adequately accurate.

APPENDIX D: ITEMS DEVELOPED BUT NOT USED IN PHASE I

Tensile ball seat

A spherical seat to compensate for minor imperfections in tensile specimens was built, but because of delay in fabrication some universal joint couplings were actually used for the tests. The tensile ball seat is shown in Figures D1 and D2.

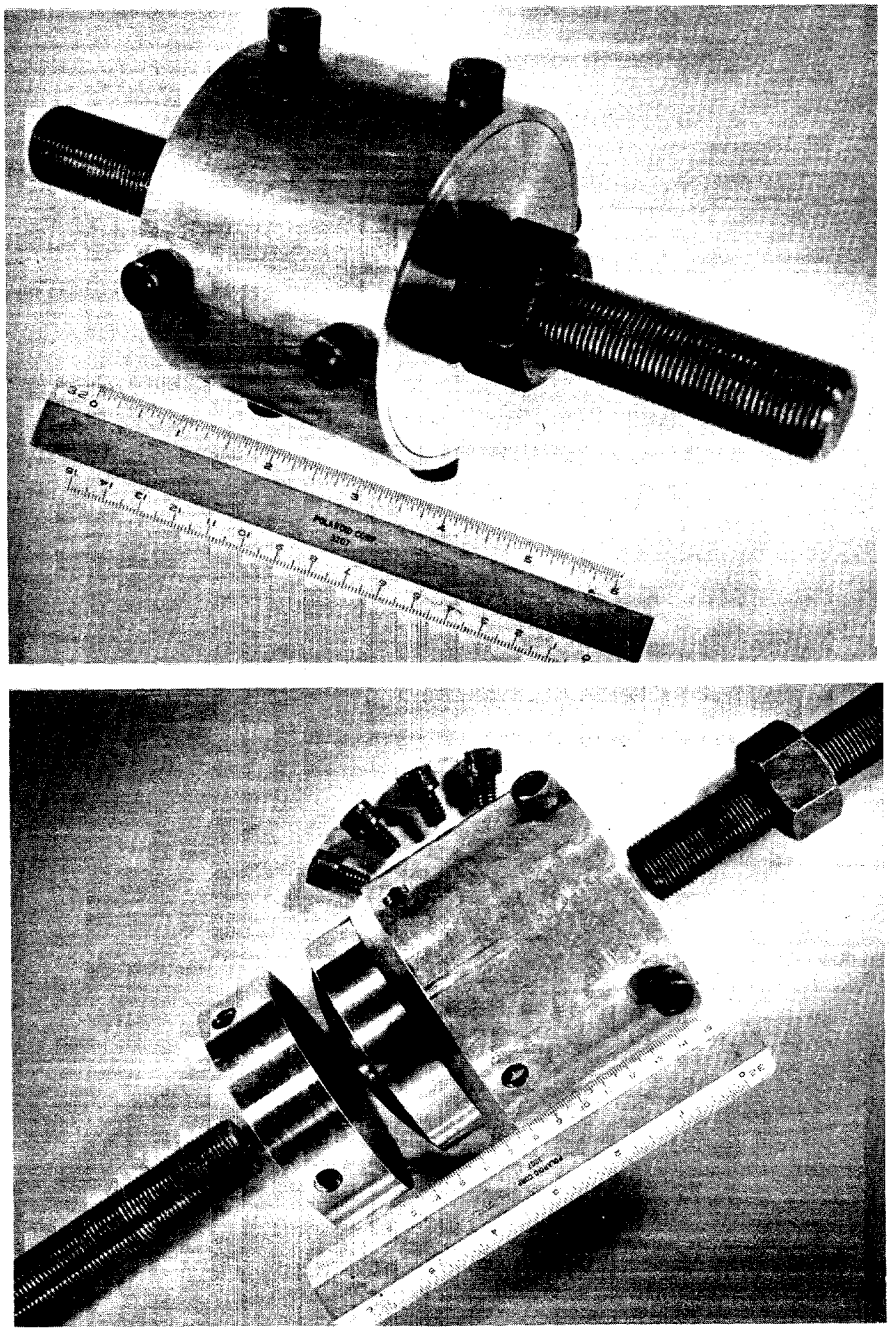

Figure D1. Tensile ball seat.

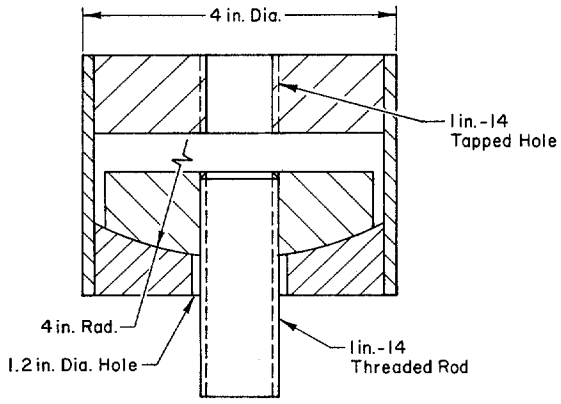

Figure D2. Dimensions of tension ball seat.

Self-centering instrument support

As explained earlier, there is a problem in supporting gauges that have to be located at the midplane of a test specimen, since the distance between the midplane and the specimen ends changes during a test. A number of mechanisms were devised to support measuring equipment at the same level as the specimen midplane. Figure 25 shows the preferred device, which uses hydraulic principles. Figure D3 gives schematics of mechanical linkages that achieve the same end.

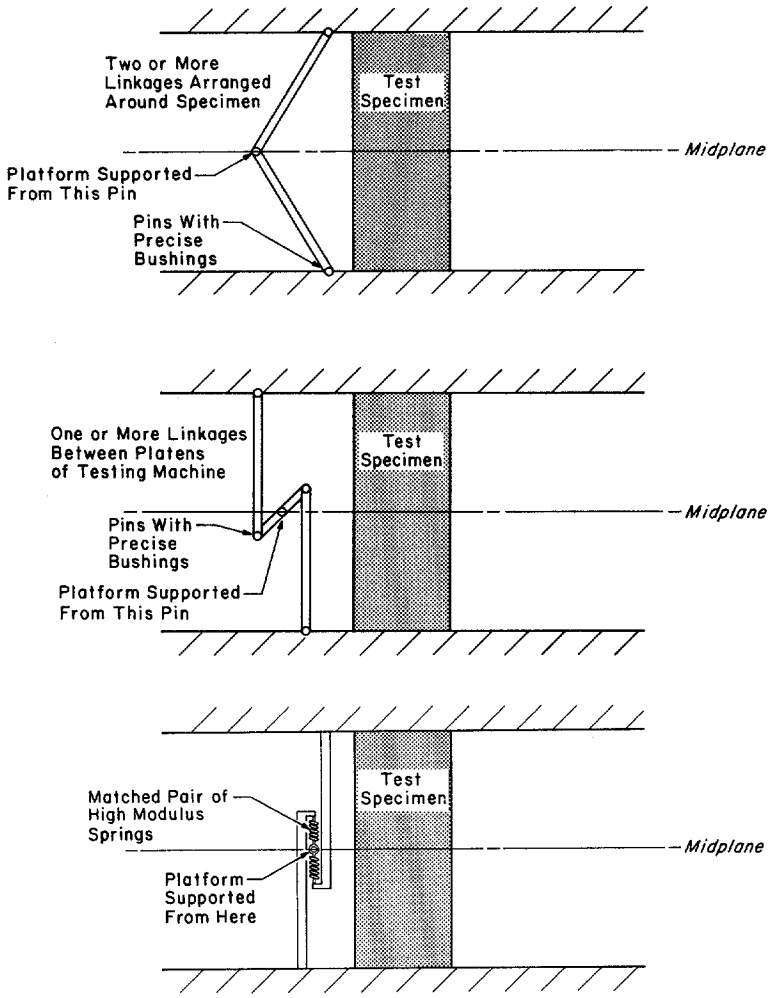

Figure D3. Mechanical linkages for supporting instruments at the level of the specimen midplane.

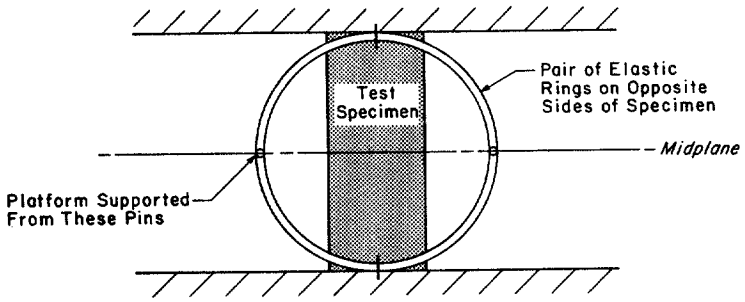

Figure D3. (cont'd).

Caliper for measuring radial strains

To avoid the clutter that exists when a radial strain yoke (Fig. 20) is used with multiple axial displacement transducers, a scissors-type caliper was considered. Figure D4 shows a relatively crude prototype made from plastic. Sharp pins on the open jaw engage the specimen, and displacement is measured at the other end of the "scissors" by a short-stroke DCDT. The end carrying the DCDT is supported by a long rubber band of low modulus.

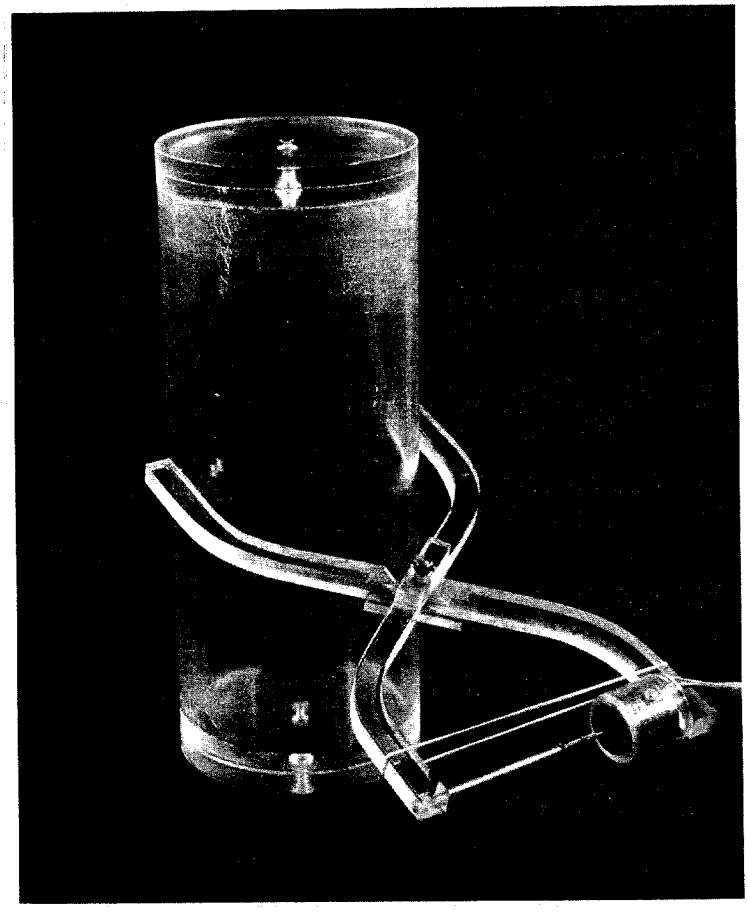

Figure D4. Scissors-type caliper for measuring radial strains.

APPENDIX E: USE OF THE BRAZIL TEST

Justification

To check on the effects of storing and shipping sea ice specimens, CRREL suggested that the Brazil test might be used. This requires some explanation, since earlier studies sponsored by CRREL showed that, while the Brazil test gives a good measure of uniaxial tensile strength for typical rocks, it does not measure the uniaxial strength of ice (Mellor and Hawkes 1971). If the Brazil test results are analyzed and interpreted in the conventional way, the "Brazil strength" for ice is several times smaller than the uniaxial tensile strength.

The Brazil test is only valid if the test material is linearly elastic, but this condition can be met if the test is sufficiently fast. Under elastic conditions, diametral compression of a disk or cylinder produces a stress field that gives a maximum tensile stress at the center. The magnitude of this tensile stress is $2P/\pi dt$, where P/t is the applied force per unit length and d is the specimen diameter. The direction of this (principal) stress is at right angles to the loading direction. However, at the center of the disk or cylinder there is also a compressive principal stress in the loading direction. The compressive stress has a magnitude of $6P/\pi dt$, i.e. $\sigma_1/\sigma_3 = 1/3$.

If the test specimen fails in splitting by a crack that initiates at the center, then the test is a biaxial strength test with $\sigma_1/\sigma_3 = 1/3$. For materials that conform to a Griffith-type failure criterion, with $\sigma_C/\sigma_T \geq 8$, a biaxial stress field with $\sigma_1/\sigma_3 = 1/3$ is just at the limit of the conditions where failure will occur at $\sigma_1 = \sigma_T$. However, ice is not a Griffith-type material because $\sigma_C/\sigma_T < 8$ at the highest loading rates commonly used in testing. Thus we must expect that failure of ice in the Brazil test will be influenced by the compressive stress component.

The chief justification for using the Brazil test to check on storage and shipping effects is that the test is easy and readily reproducible. In this application it is only required to provide a self-consistent index of strength. It would, of course, be desirable to obtain something more than an ill-defined strength index, and therefore we should try to apply the test in such a way that it gives data for failure in a defined biaxial stress field. This is possible if failure of the disk initiates at the center of the specimen, but because of the low value of σ_C/σ_T for ice, failure may initiate somewhere off-center (Mellor and Hawkes 1971, pp. 193-195).

No matter how the test data are to be used, it is essential to control the contact stresses where load is applied to the disk (Mellor and Hawkes 1971, pp. 202-209).

Design of jig for Brazil tests

The design follows the method outlined by Mellor and Hawkes (1971, pp. 207-208) using test data for ice on p. 215 to estimate probable failure forces.

For a final contact arc of approximately 8° against bare ice, $2a/R_S \approx 1/7$. With R_S (specimen radius) of 2.1 in., $2a = 2.1/7 = 0.3$ in.

For Poisson's ratio of ice and steel, we take $\upsilon_i = \upsilon_{steel} \approx 0.3$. For Young's modulus we take $E_{stainless\ steel} \approx 28 \times 10^6$ lbf/in.^{2} and $E_{ice} \approx 3$ GPa $\approx 0.435 \times 10^6$ lbf/in.^{2} (effective value).

On p. 215, Figure 28 gives a high rate value for $2KP/\pi dt$ of approximately 60 lbf/in.^{2} Since $K = 1.0$

$$\frac{2P}{\pi dt} \approx 60 \text{ lbf/in.}^2$$

or

$$\frac{P}{t} \approx \frac{60}{2} \times \pi d = 94.25\, d\ .$$

For $d = 4.2$ in., $P/t \approx 2000$ lbf/in. However, Brazil tests on ice do not measure the uniaxial tensile strength directly. When Brazil tests were used by SIPRE in the 1950s, the values of $2P/\pi dt$ were multiplied by a factor of 6 to get a value that was accepted as tensile strength. The rationale was that small imperfections represented an infinitely small hole at the center of the specimen, so that the Brazil test was really a ring with a very small hole. This suggests that P/t might be about 2000/6 = 330 lbf/in., which is a reasonable agreement with the value given by the data of Mellor and Hawkes.

Substituting these values into eq 20 on p. 207 gives

$$R_j = -2.336 \text{ in.}$$

i.e. the jaw diameter is 4.67 in. (concave).

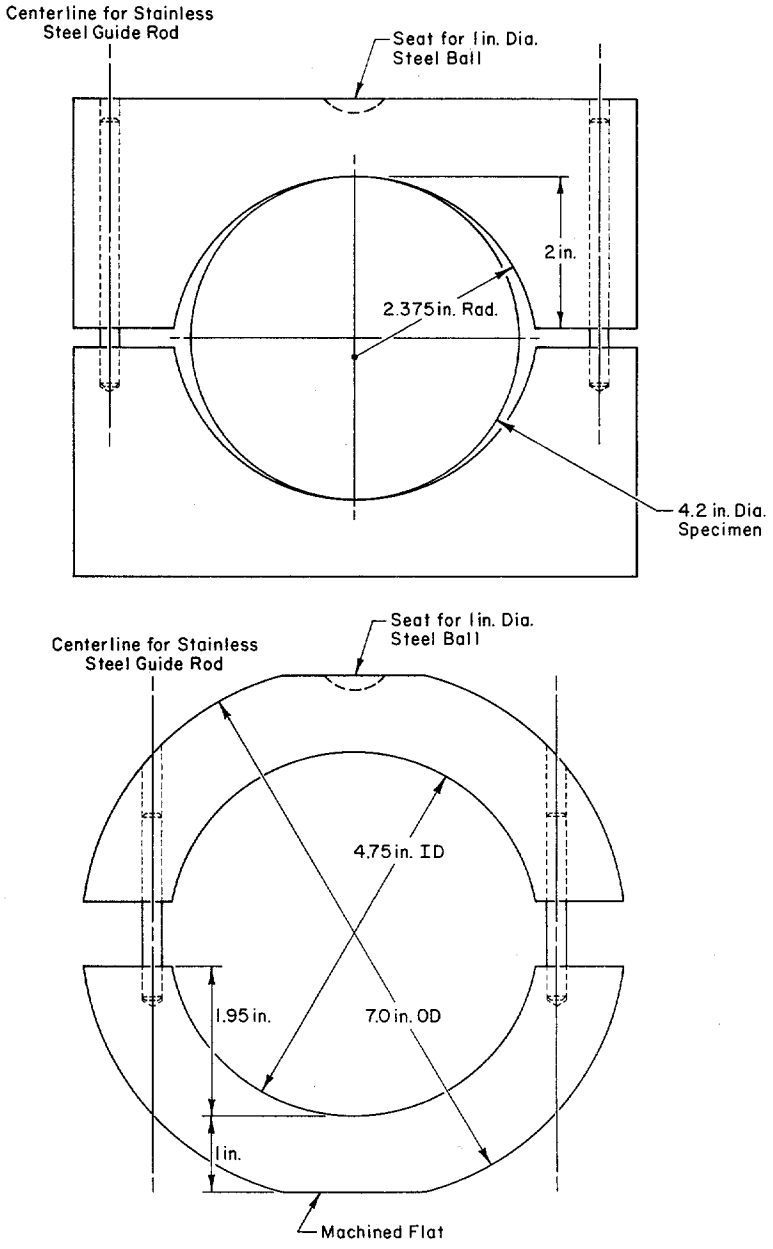

Figure E1. Loading frame for making diametral compression tests.

In going through this design calculation, we deliberately attempted to arrive at a jaw radius that is greater than the theoretical optimum value. The effective modulus of ice was taken as 3 GPa instead of the Young's modulus value of 9 GPa, and $2a/R_s$ was taken as $1/7$ instead of the theoretical optimum value of ¼. This was done because we are not dealing with perfectly machined cylinders, but with "bumpy" core, which may have some minor crushing in the contact zones. We also propose to use interface cushions (plastic or paper tape). If the jaw radius is too tight, the jig could grip the specimen and adversely affect conditions in the test section. We have also rounded up the calculated value to arrive at a final jaw diameter of 4.75 in.

Following considerations set out by Mellor and Hawkes (1971, pp. 211-212), the specimen thickness t has been chosen as $t = d/2 \approx 2.1$ in.

Because the jig will be used in the field for testing saline ice, it should be made from stainless steel. Because of the cost and availability of material, the jig will be made from round stock (Fig. E1a) instead of thick plate (Fig. E1b).

The apparatus for loading the jig and for recording data is considered separately.

A facsimile catalog card in Library of Congress MARC format is reproduced below.

Mellor, M.
Mechanical properties of multi-year sea ice: Testing techniques / by M. Mellor, G.F.N. Cox and H. Bosworth. Hanover, N.H.: Cold Regions Research and Engineering Laboratory; Springfield, Va.: available from National Technical Information Service, 1984.
iv, 43 p., illus.; 28 cm. (CRREL Report 84-8.)
Bibliography: p. 23.
1. Ice. 2. Ice properties. 3. Mechanical properties. 4. Sea ice. 5. Test techniques. I. Cox, G.F.N. II. Bosworth, H. III. United States. Army. Corps of Engineers. IV. Cold Regions Research and Engineering Laboratory, Hanover, New Hampshire. V. Series: CRREL Report 84-8.